Australia's National
Science Agency

MD-WERP Deliverable T.8b.4

Summary Report – Year 2

Project RQ8b: Groundwater as an adaptation option to current water resources management

Rojas R, González D, Fu G, Clark S and Falez E

31 May 2023

Australian Government

Murray–Darling Water & Environment Research

Citation

Rojas R, González D, Fu G, Clark S and Falez E (2023) Summary Report – Year 2 Project RQ8b: Groundwater as an adaptation option to current water resources management. MD-WERP Deliverable T2.8b.4, CSIRO, Australia.

Contents

Figures

Tables

Executive summary

This report summarises progress in the second year of the MD-WERP Project RQ8b: Groundwater as an adaptation option to current water resources management in the Murray-Darling Basin (MDB). Research continues to focus on the eight main alluvial aquifer systems comprising 22 resource units that account for 75% of groundwater extraction in the Basin. Four main activities are discussed: aquifer resilience, stress and sustainability analysis for the main alluvial aquifers of the MDB, b) cluster analysis of groundwater level trends and causal attribution; c) a framework for stochastic assessment of managed aquifer recharge (MAR) potential, and d) a framework to assess potential evaporative savings realised by using infiltration-based storage compared to surface storage.

Eleven groundwater resource units where potential resilience, stress and sustainability issues, or a combination of these, were identified. A comprehensive indicator-based assessment illustrates the advantage of analysing these issues simultaneously in the alluvial aquifers of the MDB. This assessment highlights the opportunities for groundwater to help improving water management in the MDB, anchored on concepts of aquifer resilience, stress, and sustainability by targeting specific aspects such as declining groundwater level trends, groundwater salinity, occurrence of Groundwater Dependent Ecosystems, among others, at specific groundwater resource units.

We improved our understanding on the groundwater level trends observed in the alluvial aquifers of the MDB by employing clustering techniques (Hierarchical Cluster Analysis, HCA and Self-Organising Maps, SOMs) to disentangle trend patterns in groundwater levels spatially and temporally. Similarly, we employed artificial intelligence/deep learning techniques (recurrent neural network) to infer causal attribution to these patterns using a series of covariates such as precipitation, potential evaporation, pumping infrastructure, groundwater usage. Results show that both clustering techniques identified six dominant patterns with comparable performance, thus indicating these patterns are robust and properly identified from the dataset (910 observations bores). Differences arose in the number of time series allocated to each cluster, however a geographical analysis indicated that this was the result of time series within specific areas being attributed to closely related patterns. Similarly, the temporal analysis shows the impact of the Millennium Drought on declining and recovering patterns post-drought.

A causal attribution framework based on neural network models is presented to determine the main contributors to changes in groundwater level patterns given climate and anthropogenic conditions. These models will be probed to determine which driving factors are impacting the groundwater level trends the most. It is possible to investigate these attributions temporally as well as spatially, to determine if the main factors contributing to altered groundwater levels have transformed over the period of study. Improvements to the current data set, and therefore the modelling results, could include using rain, PET, and groundwater use information on a local basis rather than at the resource unit level. Accessing spatially and temporarily comprehensive data on groundwater use will largely determine the quality of the causal inference under anthropogenic conditions.

The proposed framework for the assessment of MAR potential across the main alluvial resource units of the MDB adopts a Monte Carlo approach to capture uncertainties in inputs and assumed feasibility thresholds. Preliminary results illustrate the outputs generated with the assessment methodology for unconfined aquifer conditions, and methods will be developed for confined aquifer conditions. A key input dataset to confined and unconfined assessment is the available height for recharge and storage. The study will test the feasibility of using groundwater level trend magnitudes generated through other tasks of RQ8b as a basis for interpolation to capture temporal dynamics in groundwater levels and avoid assumptions of maximum allowable water level rise. The resulting outputs will guide the conceptualisation of potential MAR sites for preliminary financial assessment.

The potential savings that could be realised by using sub-surface storage in suitable locations where surface storage may have limited efficiency is explored using a suite of hydrological time series calculations. An example for the Namoi region based on the dimensions of Lake Keepit and typical farm dam designs compared to infiltration basins with low and high infiltration rates is presented. Results indicate significant evaporative savings through MAR compared with equivalent surface storage. Evaporation losses reported here should not be interpreted as actual potential losses from reservoirs or farm dams under normal operation, as water use is ignored. Replicating these calculations across different hydrological and climate zones and for different dam and infiltration basin characteristics will provide more insight into where MAR can offer potential benefits over equivalent surface storage.

Activities for the third year of project RQ8b will expand our knowledge on devising and implementing a framework to assess MAR economic feasibility as an adaptation option to improve groundwater management. This will focus on reducing uncertainty around the costs of MAR at different scales and operating conditions. Previous RQ8b activities on aquifer resilience, stress and sustainability, in combination with MAR feasibility mapping, will inform one or more conceptual MAR site configurations. An existing tool will be used to estimate the range of costs expected to implement a conceptual MAR scheme. Policy and regulatory principles needed to enable the implementation of a MAR scheme will be discussed depending on the scale and objective of the conceptualised scheme and potential ownership and governance arrangements.

1 Introduction

Project RQ8b focuses on using groundwater as an adaptation option for water resource management centred on the eight main alluvial aquifer systems comprising 22 resource units that account for around 75% of annual groundwater extraction on average (2013-13 to 2018-19) in the Basin (MDBA, 2020b). It consists of three one-year activities. In the first year, Activity 8b.1 aimed to enhance our knowledge of groundwater level trends, usage patterns, and relevant alluvial aquifers in the Murray-Darling Basin (MDB). The primary objective was to identify areas where groundwater plays a significant role and discover opportunities for maximising its potential to improve economic, social, and environmental outcomes in the MDB.

In Year 2, Activity 8b.2 builds upon the findings of Year 1 to investigate patterns of temporal and spatial clustering in observed groundwater level trends, and to explore the potential factors driving such patterns. Additionally, Year 2 activities delve deeper into concepts related to aquifer resilience, stress, and sustainability in the alluvial systems of the MDB.

This report presents a detailed analysis of potential issues related to these concepts, supported by twelve metrics calculated at groundwater sustainable diversion limit (SDL) resource unit scale. Furthermore, we introduce a Monte Carlo framework to assess managed aquifer recharge (MAR) potential in the main alluvial aquifers of the MDB. This framework utilizes variable screening thresholds and combines physical features (e.g., alluvial thickness), binary screening of physical features, groundwater level trends, and porosity estimates to calculate the likelihood that an aquifer can receive a certain infiltration volume while fulfilling specific distance and depth criteria from the river or irrigation areas. Lastly, we propose a conceptual framework to evaluate evaporation savings when infiltration-based MAR storage is implemented in comparison to equivalent surface storage.

1.1 Scope of RQ8b: Groundwater as an adaptation option to current water resources management

During the second year the scope of activities was twofold: expand and consolidate our understanding of spatial and temporal patterns in groundwater level trends in the main alluvial aquifers of the MDB and provide foundational analysis of managed aquifer recharge as an adaptation option to water resources management in the MDB. During the second year the project aimed to:

- Apply advanced clustering techniques to unravel the patterns observed in groundwater levels trends during year 1 activity,
- Compare clustering techniques in terms of performance and identify spatial and temporal patterns in the groundwater level trends,
- Explore causal attribution to explain patterns in groundwater level trends,

- Explore a Monte Carlo framework to assess the MAR potential in the main alluvial aquifers of the MDB based on physical features such as alluvial thickness, porosity, depth to standing water level trends, clay content, distance to rivers/irrigation areas,
- Propose a conceptual framework based on simplified water balance calculations to assess the evaporation savings due to infiltration-based MAR compared to equivalent surface storage.

Additionally, as legacy task from Year 1 we deepened our understanding on the resilience, stress and sustainability of alluvial aquifers by proposing and using an index-based framework underpinned by twelve groundwater-related metrics.

1.2 Groundwater use across the Murray-Darling Basin

Close to 75% of the groundwater use in the MDB for the period 2012-2019 is concentrated in eight alluvial systems (Figure 1), with more recent estimates bringing this value closer to 80%. Within each of the main alluvial aquifers, specific groundwater resource units show the following pattern in groundwater usage:

- **Condamine** (Upper Condamine Alluvium – Central GS64a[1], – Tributaries GS64b). For the period 2012-13 until 2018-19 this alluvial system concentrates on average 43% of the total groundwater use metered in SDL resource units of Queensland, with the most recent estimate bringing this value close to 50%. If groundwater use in the Upper Condamine Basalts (GS65) is also included, the average use amounts to 80% of groundwater use in Queensland.
- **Gwydir** (Upper Gwydir, GS43 – Lower Gwydir, GS24). For the period 2012-13 until 2018-19 this alluvial system concentrates on average 4% of the total groundwater use metered in SDL resource units of New South Wales.
- **Namoi** (Upper Namoi, GS47, GS48 – Lower Namoi, GS29). For the period 2012-13 until 2018-19 this alluvial system concentrates on average 18% of the total groundwater use metered in SDL resource units of New South Wales.
- **Macquarie** (Upper Macquarie, GS45 – Lower Macquarie, GS26). For the period 2012-13 until 2018-19 this alluvial system concentrates on average 5% of the total groundwater use metered in SDL resource units of New South Wales.
- **Lachlan** (Upper Lachlan, GS44 – Lower Lachlan, GS25). For the period 2012-13 until 2018-19 this alluvial system concentrates on average 16% of the total groundwater use metered in SDL resource units of New South Wales.
- **Murrumbidgee** (Lower Murrumbidgee Shallow, GS28a – Lower Murrumbidgee Deep, GS28b – Mid-Murrumbidgee, GS31). For the period 2012-13 until 2018-19 this alluvial system concentrates on average 29% of the total groundwater use metered in SDL resource units of New South Wales.

[1] This nomenclature corresponds to the 80 Groundwater Sustainable Diversion Limits (SDL) Resource Units reported by the Murray-Darling Basin Authority (https://data.gov.au/data/dataset/66e3efa7-fb5c-4bd7-9478-74adb6277955. Accessed on 15-November-2021).

- **Murray** (Lower Murray Shallow, GS27a – Lower Murray Deep, GS27b – Upper Murray, GS46). For the period 2012-13 until 2018-19 this alluvial system concentrates on average 8% of the total groundwater use metered in SDL resource units of New South Wales.
- **Goulburn-Murray** (Shepparton Irrigation Region, GS8a – Sedimentary Plain, GS8c). For the period 2012-13 until 2018-19 this alluvial system concentrates on average 88% of the total groundwater use metered in SDL resource units of Victoria, with the most recent estimate bringing this value to 90%.

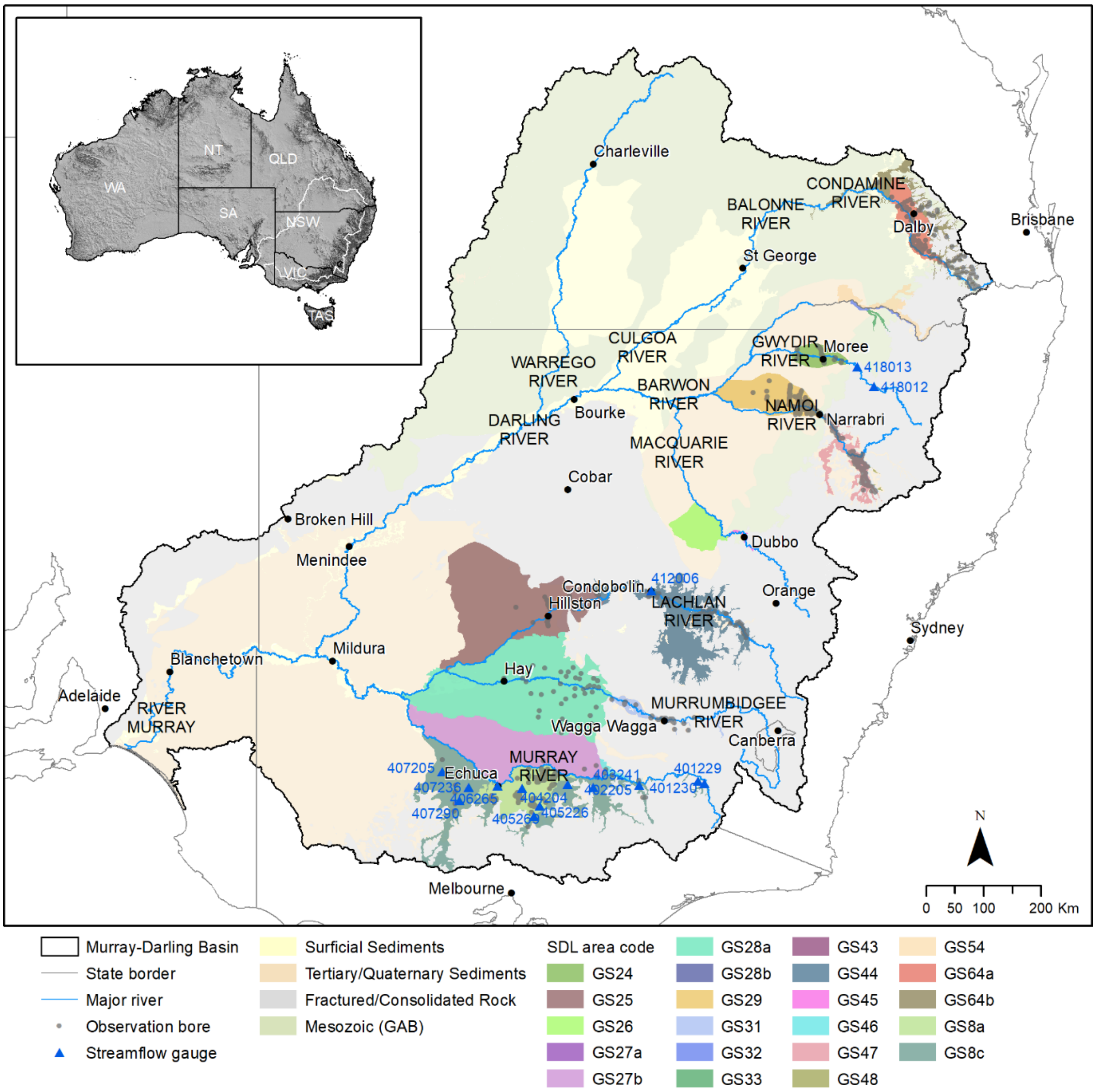

Figure 1 Main alluvial systems in the Murray-Darling Basin and the corresponding groundwater SDL resource units (from https://www.mdba.gov.au/publications/products/groundwater-alluvial-areas-map, accessed 12/11/2021). Map includes Border Rivers groundwater resource units for consistency with Barron et al. (2011).

Reported groundwater use in the resource units comprising these major alluvial aquifers and the Border Rivers is presented in Table A.1 in the appendix.

2 Groundwater resilience, stress and sustainability of the alluvial aquifers of the Murray-Darling Basin

This section is based on a research article published in the Journal of Hydrology: Regional Studies: Rojas, R., Gonzalez, D. and Fu, G. (2023) Resilience, stress and sustainability of alluvial aquifers in the Murray-Darling Basin, Australia: opportunities for groundwater management. *Journal of Hydrology: Regional Studies, 47, 101419, doi:10.116/j.ejrh.2023.101419.* The following sections contain a summary of the main methods and results published in this article.

2.1 Scope

Research on aquifer vulnerability, sensitivity (Rine et al., 2006; Watson et al., 2020) and potential (Mukherjee et al., 2012) has primarily focused on assessing pollution risk and spatial vulnerability (Butler, 2010; Rine et al., 2006). However, there has been a growing interest in understanding groundwater resources from a systemic lens by exploring concepts such as resilience, stress, and sustainability (Akbar et al., 2022; de la Hera-Portillo et al., 2021; Elshall et al., 2020; Gleeson et al., 2020, 2012; Majidipour et al., 2021; Richey et al., 2015a, 2015b). With few exceptions (e.g. Akbar et al., 2022), research has focused mainly on the individual evaluation of these concepts using index-based assessment. In this section, we simultaneously explored and applied the concepts of groundwater resilience, stress and sustainability in the main alluvial aquifers of the Murray-Darling Basin (MDB) to obtain a systemic view of groundwater resources.

Recent literature reviews show the relevance of the MDB in terms of environmental, socioeconomic, hydrological and water management aspects in the last decades (Hart et al., 2020; Leblanc et al., 2012; MDBA, 2020a; Ross, 2012; Stewardson et al., 2021; Walker et al., 2020; Williams, 2011). However, a regional basin-scale analysis on the main alluvial aquifers of the MDB anchored on the concepts of groundwater resilience, stress and sustainability is currently missing. To address this issue, we analysed aspects related to long-term groundwater level trends, metered groundwater usage, groundwater salinity, storage volumes, recharge rates, aquifers' buffering capacity to absorb changes in recharge rates, and the occurrence and diversity of Groundwater Dependent Ecosystems (GDEs). The aim of our work is to provide a systemic overview of the alluvial aquifers of the MDB anchored in concepts of groundwater resilience, stress and sustainability to identify potential opportunities to improve groundwater management. To achieve this, we combine three lines of evidence: a) long-term trend analysis of groundwater levels; (b) calculation of the groundwater footprint (GF) considering both volume (Gleeson et al., 2012) and quality (salinity) (Kourgialas et al., 2018); and (c) an explicit comparison among groundwater resource units aligning with the most recent definition of groundwater sustainability (Elshall et al., 2020; Gleeson et al., 2020).

2.2 Methods

We embraced the concepts of groundwater resilience, stress and sustainability by merging three lines of evidence: a) long-term trend analysis of groundwater levels, b) insights on groundwater stress, and c) a systematic comparison among the groundwater resource unit regarding size of the resource, groundwater usage, storage, buffering capacity to recharge changes, and the presence and diversity of GDEs (Figure 2). Each proxy analysed was assessed using four indicators:

1. Resilience: mean and maximum groundwater level trends at resource unit scale, number of wells showing statistically significant declining trends in groundwater levels, and relative groundwater depletion rate defined as the ratio between total storage and change in storage from groundwater level trends compared across resource units.
2. Stress: groundwater footprint/stress based on Gleeson et al. (2012), and integrated groundwater footprint/stress based on Kourgialas et al. (2018) for three salinity classes (brackish, saline and highly-saline) defined by MDBA (2020a).
3. Sustainability: development, responsiveness and numerical relevance scores and an ordination approach based on Barron et al. (2011) to identify relevant groundwater resource unit.

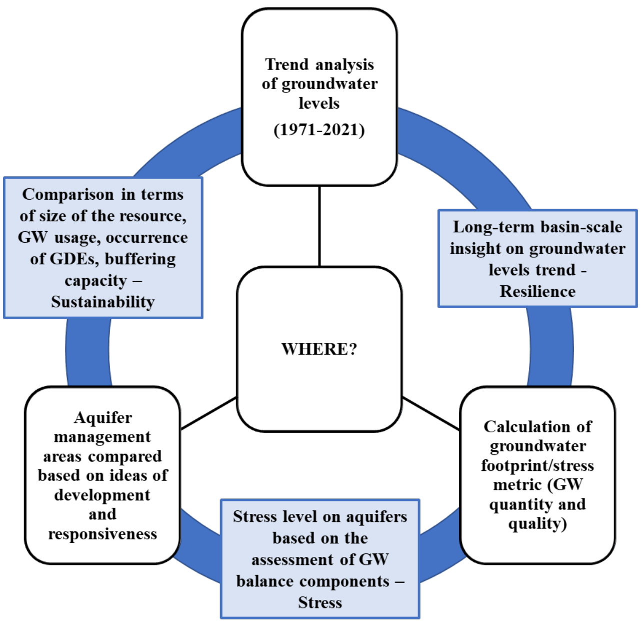

Figure 2 Framework anchored in the concepts of aquifer resilience, stress and sustainability and proxies used to analyse these concepts (from Rojas et al. (2023)).

2.2.1 Trends in groundwater levels of alluvial aquifers

We built upon the long-term trend analysis on groundwater levels for the alluvial aquifers of the MDB described in Fu et al. (2022) to frame the analysis around groundwater resilience (de la Hera-Portillo, 2021). Trends were analysed for 910 observation bores within resource unit areas with at least two annual groundwater level measurements in the period 1971-2021 (shown in Figure 1). Data on depth to standing water level (DTW) was accessed from the National Groundwater

Information System (NGIS) v1.7.0 (updated in July 2021). Out of the 22 groundwater resource units analysed (Figure 1), 14 fulfilled the following criterion: at least two measurements per year for a 40-year period. Fu et al. (2022) describe the data selection and filtering process in detail whereby drilled depth was used to select bores within the estimated thickness of the alluvium and separate bores in shallow and deep resource units according to approximate depth thresholds. Bore records did not have aquifer attribution so results aggregated at resource unit level may contain trends from bores in different layers or zones within resource units. Similar limitations exist for all data reported at resource unit level, e.g. extraction limits and actual take.

Three trend analysis methods, namely, Kendall/Sen's slope (Hirsch et al., 1982), linear slope, and two-period comparison/Innovative Trend Analysis (ITA) (Dong et al., 2020; Şen, 2012) were applied on the annual minimum, maximum and average DTW. For details on the trend analysis methods the reader is referred to Fu et al. (2022). Basin-scale average long-term trends for DTW were obtained for each resource unit and a series of statistics (e.g. mean trends, max trends, no. of wells showing statistically significant trends, groundwater depletion rate) were calculated to identify a subset of resource units showing groundwater resilience issues.

2.2.2 Groundwater Footprint/Stress

The groundwater footprint (GF) was calculated as (Gleeson et al., 2012):

$$GF = A\left[\frac{C}{(R-E)}\right] \quad [1]$$

where *A* is the areal extent of the region of interest (e.g. aquifer management area) (L^2), *C* is the annual groundwater abstraction/use (L^3/T), *R* is the annual recharge rate (L^3/T), and *E* is the groundwater contribution to environmental streamflow (L^3/T). Gleeson et al. (2012) and Mahdavi (2021) suggest alternative ways to calculate *E*, for example, hydro-ecological studies, direct measurements of springs, hydrological modelling results, expert elicitation/judgement, expressed as a fraction of recharge, or as a low-flow statistic, e.g., Q95, Q90/Qavg, as defined by Smakhtin et al. (2004). Groundwater contribution to environmental streamflow (E) was obtained from either: (1) available modelling results (MDBA, 2020a); (2) reports describing groundwater contributions to streamflow (NSW-DPIE, 2019a; NSW-DPIE, 2019b; Welsh et al., 2014); (3) or by estimating the Q95, Q90/Qavg statistics from representative gauging stations. For the latter we used a spatial dataset describing the groundwater-surface interactions to identify river reaches and suitable gauging stations where contributions from groundwater to streamflow are expected in Shepparton Irrigation Region (GS8a) and Goulburn Sedimentary Plain (GS8c) (VIC-DELWP, 2020) (see Figure 1).

2.2.2.1 Salinity and groundwater stress

We included groundwater quality aspects using a revised version of the groundwater footprint proposed by Kourgialas et al. (2018) and defined as:

$$iGF = GF \times \left(1 + n\left[CF_1\frac{A_1}{A} + CF_2\frac{A_2}{A} + \cdots + CF_n\frac{A_n}{A}\right]\right) \quad [2]$$

where, *GF* is the groundwater footprint as defined in equation [1], *n* is the number of contaminants in the aquifer system, $CF_{1\ldots n}$ is a factor for contaminant (j), with j=1,…,n, with CF_j

equal to 1 if the contaminant is present or above a threshold and zero otherwise, $A_{1...n}$ is the extent of the contaminated area, and A is the areal extent of the region of interest.

We used groundwater salinity data from 12,513 observation bores from the NGIS to calculate *iGF* in the 22 groundwater resource units analysed (Table 1). Upper and lower two percent of salinity data were removed to filter out extreme values. From the remaining data, the 95th percentile salinity value was calculated for each bore for use in spatial interpolation. There were no salinity data in the Upper Gwydir GS43, sparse in the Lower Murrumbidgee Shallow Alluvium GS28a, and poorly distributed across the Lower Murray Shallow Alluvium GS27a. These groundwater resource units were therefore excluded from spatial interpolation. Interpolation across the Border Rivers resource units included 36 bores in total although were unevenly distributed. A range of kriging interpolation model and parameter combinations were tested to create prediction surfaces of salinity. Model fit was assessed using cross-validation. The semi-variogram model and parameter combination that minimised root-mean-square error (RMSE) was selected. A separate kriging model was applied in the Shepparton Irrigation Region (SIR) (GS8a) as it overlaps and has variable hydraulic connection with the underlying Sedimentary Plain (GS8c).

Table 1 Salinity data summary for SDL resource units and kriging model performance

SDL resource unit	Code	No. bores	Area km2	p95 min (µS/cm)	p95 max (µS/cm)	Kriging model	Range (km)	RMSE (µS/cm)
Goulburn-Murray: SP	GS8c	1760	21928.92	260	35213	Circular	20.4	4464
Goulburn-Murray: SIR	GS8a	10800	6579.87	255	35244	K-Bessell	5.1	4893
Lower Gwydir Alluvium	GS24	121	2340.39	280	6168	Circular	20.4	4464
Lower Lachlan Alluvium	GS25	95	25282.63	265	32425	Circular	20.4	4464
Lower Macquarie Alluvium	GS26	92	3960.96	302	33325	Circular	20.4	4464
Lower Murray Deep Alluvium	GS27b	73	17803.16	280	31135	Circular	20.4	4464
Lower Murray Shallow Alluvium	GS27a	61	17803.16	278	35100	na	na	na
Lower Murrumbidgee Deep Alluvium	GS28b	90	32437.91	260	15046	Circular	20.4	4464
Lower Murrumbidgee Shallow Alluvium	GS28a	5	32437.91	298	3337	na	na	na
Lower Namoi Alluvium	GS29	227	7115.07	291	29700	Circular	20.4	4464
Mid-Murrumbidgee Alluvium	GS31	142	1472.68	263	13920	Circular	20.4	4464
NSW Border Rivers Alluvium	GS32	8	365.98	320	2097	Circular	20.4	4464
NSW Border Rivers Tributary Alluvium	GS33	3	248.62	632	1028	Circular	20.4	4464
Queensland Border Rivers Alluvium	GS54	25	25282.63	439	5306	Circular	20.4	4464
Upper Condamine Alluvium (CCA)	GS64a	148	4346.05	486	25061	Circular	20.4	4464
Upper Condamine Alluvium (Trib.)	GS64b	78	3777.73	517	25350	Circular	20.4	4464
Upper Gwydir Alluvium	GS43	0	97.37	Na	Na	na	na	na
Upper Lachlan Alluvium	GS44	138	12962.72	294	30775	Circular	20.4	4464
Upper Macquarie Alluvium	GS45	51	273.17	262	23990	Circular	20.4	4464
Upper Murray Alluvium	GS46	13	489.42	666	2675	Circular	20.4	4464
Upper Namoi Alluvium	GS47	337	3573.04	267	23700	Circular	20.4	4464
Upper Namoi Tributary Alluvium	GS48	6	56.36	878	1428	Circular	20.4	4464

Continuous predicted values were contoured into salinity classes TDS (mg/L) following the Recharge Risk Assessment Method (RRAM) described in MDBA (2020): 1) fresh <1500 mg/L, 2) brackish 1500–3000 mg/L, 3) saline 3000–14,000 mg/L, and 4) highly saline >14,000 mg/L. The total areas of these salinity classes within each groundwater resource unit were used as inputs to calculate *iGF* in equation 2.

The ratio of both *GF* and *iGF* by the resource unit is interpreted as a groundwater stress metric, with GF/A >1 and iGF/A > 1 indicating unsustainable consumption of groundwater resources (Kourgialas et al., 2018).

2.2.3 Aquifer development and responsiveness

In this work, we embraced the idea by Elshall et al. (2020) suggesting that sustainability should be assessed from both aquifer performance and management perspectives. To achieve this, we employed modified versions of indicators reflecting aquifer development and responsiveness proposed by Barron et al. (2011) and Currie et al. (2010). These indicators compare different aspects such as storage volumes, current and allowable groundwater use, recharge rates, occurrence and diversity of GDEs, and buffering capacity (storage proportional to recharge), across groundwater resource units. The indicators proposed are defined as follows:

$$Development\ SDL_i = D_i = \frac{Actual\ GW\ Use_i}{Max(Actual\ GW\ Use_i\colon i=1,\dots,n)} * \frac{SDL_i}{Max(SDL_i\colon i=1,\dots,n)} * f(GDE)_i \qquad [1]$$

$$Responsiveness\ SDL_i = Re_i = \frac{Actual\ GW\ Use_i}{SDL_i} * f(R\colon S)_i \qquad [2]$$

where *i*, i=1,…,22 is the i-th groundwater resource unit, *n*=22 is the total number of SDL resource units, $Actual\ GW\ Use_i$ (ML/y) represents metered groundwater usage reported for the period 2012-2019 for the i-th groundwater resource unit, SDL_i represents the long-term average groundwater sustainable diversion limit (ML/y) associated with i-th resource unit, $f(GDE)_i$ represents a factor accounting for GDE presence and diversity in the i-th SDL, and $f(R{:}S)_i$ is a factor reflecting the buffering capacity to absorb changes in recharge rates (*R*) with respect to storage capacity (*S*) of the i-th resource unit.

Both indicators can be combined to obtain a numerical ranking following the standardization process described in Barron et al. (2011). Additionally, we employed an ordination approach (Barron et al., 2011) to rank groundwater resource units as follows: developed aquifer systems (low responsiveness and high development scores); responsive aquifer systems (low development and high responsiveness scores); and relevant aquifer systems (high development and high responsiveness scores).

In this work, we improved on the calculation of $f(GDE)_i$ in equation 1 by using the latest spatial data available from the GDE Atlas (v.2019) published by the Australian Bureau of Meteorology (BoM) (http://www.bom.gov.au/water/groundwater/gde/). The GDE Atlas contains spatial information on aspects such as GDE potential (unknown-low-moderate-high potential of interacting with groundwater), GDE ecotypes, eco-hydrogeological zones, and specific areal extents. This information was used to refine the $f(GDE)_i$ factor to obtain a more robust and representative index. To achieve this, we grouped aquatic GDEs based on ecotype (wetland, river, spring) and eco-hydrogeological zone resulting in 26 classes for aquatic GDEs. Terrestrial GDEs (one vegetation ecotype class) were grouped according to sub-ecotype resulting in 476 classes. We then adapted two widely used diversity indices, namely, Shannon and Simpson Diversity Indices (Gorelick, 2006; Spellerberg & Fedor, 2003) to use class areas instead of species counts within each groundwater resource unit. These diversity indices were calculated on filtered GDE data to exclude areas defined as ‘low’ or ‘unknown’ GDE potential for connection to groundwater and were weighted by the ratio between GDE area and total resource unit (AreaGDE/AreaSDL) to account for the spatial relevance of GDEs.

The factor $f(R{:}S)_i$ is expressed as a membership function as follows:

$$f(R:S) = \begin{cases} 0.9 & high\ R:S \\ 0.3 & moderate\ R:S \\ 0.01 & low\ R:S \end{cases} \qquad [3]$$

To define the three classes (high, moderate and low R:S ratios), we used recharge estimates reported in the literature and average values of standing water levels, aquifer base level, planar areas, aquifer types, and estimates of porosity for storage calculations mostly from background documentation of Water Sharing Plans (WSP) (MDBA, 2020; DNRME, 2018; McNeil et al., 2018; MDBA, 2020; OGIA, 2016; Water, 2015; Welsh et al., 2014). For the groundwater resource units in Queensland and Victoria, we used the depth of regolith digital product (Wilford et al., 2018).

2.3 Results

Table 2 shows the statistics obtained from the trend analysis for 14 groundwater resource units with available data. Grey cells indicate those resource units where the (mean or maximum) groundwater level trend for the period 1971/2021 is above average across all resource units (0.11 and 0.43 m/y, respectively), or where the number of observation bores showing statistically significant decreases in DTW is greater than 80%. Except for Lower Gwydir Alluvium, all resource units show a high proportion (> 80%) of observation bores with statistically significant decreasing trends in DTW.

Table 2 Groundwater level trend magnitudes (m/y) per SDL resource unit based on Beta value estimate (Hirsch et al., 1982; Kendall, 1975) for the mean and maximum annual DTW, number of bores showing statistically significant decreasing trends (adapted from Rojas et al. (2023)).

SDL Code	SDL Resource Units	Area Km^2	No. of wells	Mean	Max Trend (m/y)	Stat. sig. wells showing decreasing trend
GS29	Lower Namoi Alluvium	7115	155	0.19	0.68	98%
GS28b	Lower Murrumbidgee Deep Alluvium	32438	36	0.18	0.50	81%
GS47	Upper Namoi Alluvium	3573	174	0.16	0.53	95%
GS8c	Goulburn-Murray: SP	21929	55	0.15	0.59	100%
GS64a	Upper Condamine Alluvium (CCA)	4346	74	0.12	0.48	91%
GS24	Lower Gwydir Alluvium	2340	48	0.12	0.35	73%
GS31	Mid-Murrumbidgee Alluvium	1473	90	0.12	0.35	100%
GS44	Upper Lachlan Alluvium	12963	56	0.11	0.42	100%
GS27b	Lower Murray Deep Alluvium	17803	4	0.11	0.36	75%
GS25	Lower Lachlan Alluvium	25283	31	0.10	0.33	84%
GS64b	Upper Condamine Alluvium (Tributaries)	3778	73	0.06	1.01	93%
GS28a	Lower Murrumbidgee Shallow Alluvium	32438	12	0.03	0.09	67%
GS46	Upper Murray Alluvium	489	6	0.05	0.16	83%
GS8a	Goulburn-Murray: SIR	6580	96	0.04	0.21	89%

It is worth noting that the depletion rate is determined by considering the ratio of storage volume and the change in storage volume. Absolute values for the depletion rates are therefore only referential. To comparatively assess groundwater resource units in the following sections, we focus on the normalised values of the depletion rate (see section 2.4, Figure 6).

In Figure 3, the 95th percentile salinity values across all resource units are spatially interpolated, along with the corresponding salinity class areas that were used to calculate *iGF*. Most of the groundwater SDL resource units covering alluvial aquifers are classified as freshwater (54%) or brackish (18%) groundwater, while 25% are classified as saline. Highly saline areas are identified in specific regions, such as the lower sections of the Murray River in the Sedimentary Plain (GS8c), Lower Murray Deep (GS27b), and a localized area of the Shepparton Irrigation Region (GS8a). Figure 3 also indicates that most of the freshwater areas (>80% of the total SDL resource unit) are concentrated around the narrow alluvial deposits located towards the uplands of the MDB and in the Lower Gwydir Alluvium (GS24). In the Condamine Alluvium (GS64a), fresh groundwater aligns well with the Condamine River. Similarly, alluvial aquifers in the MDB's extensive alluvial plains show freshwater pockets closely aligned with the main rivers of these regions, such as Lachlan (GS25), Murrumbidgee (GS31 and GS28b), and Lower Murray Deep Alluvium (GS27b). This would suggest strong connections between surface water and groundwater for these alluvial aquifers. Brackish and saline groundwater regions are prevalent in the lower sections of the SDL resource units, such as Lower Namoi (GS29), Lower Murrumbidgee Deep (GS28b), Lower Murray Deep (GS27b), and Goulburn-Murray Sedimentary Plain (GS8c).

The *iGF* metric uses lateral extents of salinity classes for the calculation of stress levels at SDL resource unit scale. Groundwater salinity values may vary with depth however, this was not accounted for in the spatial interpolation beyond separating deep and shallow SDL resource units based on observation bore drilled depth.

Figure 4 illustrates the distribution of groundwater stress metric (*GF/A*) at the resource unit scale. The first panel (Figure 4a) represents the stress metric without considering the salinity data, which serves as a baseline for comparison. This figure assumes that all areas contribute to the calculation of the stress metric. The second panel (Figure 4b) considers areas with high salinity, including Shepparton Irrigation Region (GS8a), Goulburn-Murray Sedimentary Plain (GS8c), and Lower Murray Deep (GS27b), to calculate *iGF*. However, these areas do not significantly affect the groundwater stress metric (*iGF/A*) to values higher than one, and no changes are observed compared to the baseline (Figure 4a). The third panel (Figure 4c) considers highly saline and saline groundwater areas to calculate *iGF*. Both Lower Lachlan Alluvium (GS25) and Lower Murrumbidgee Deep Alluvium (GS28b) experience stress conditions (*iGF/A* > 1) due to the increase in areas falling under this salinity class (57% and 48% of total SDL resource unit, respectively). At the same time, Lower Gwydir Alluvium (GS24), Lower Macquarie Alluvium (GS26), and Goulburn-Murray Sedimentary Plain (GS8c) show *iGF/A* values greater than 0.8. Finally, Figure 4d includes areas with highly saline, saline, and brackish groundwater. Several resource units indicating groundwater stress are included: Lower Macquarie Alluvium (GS26), Upper Condamine Alluvium (GS64a), Upper Condamine Alluvium Tributaries (GS64b), and Goulburn-Murray Sedimentary Plain (GS8c). It is worth noting that the Shepparton Irrigation Region (GS8a) is not experiencing stress levels due to its low groundwater use, significant recharge, and the area considered in the *GF* calculation.

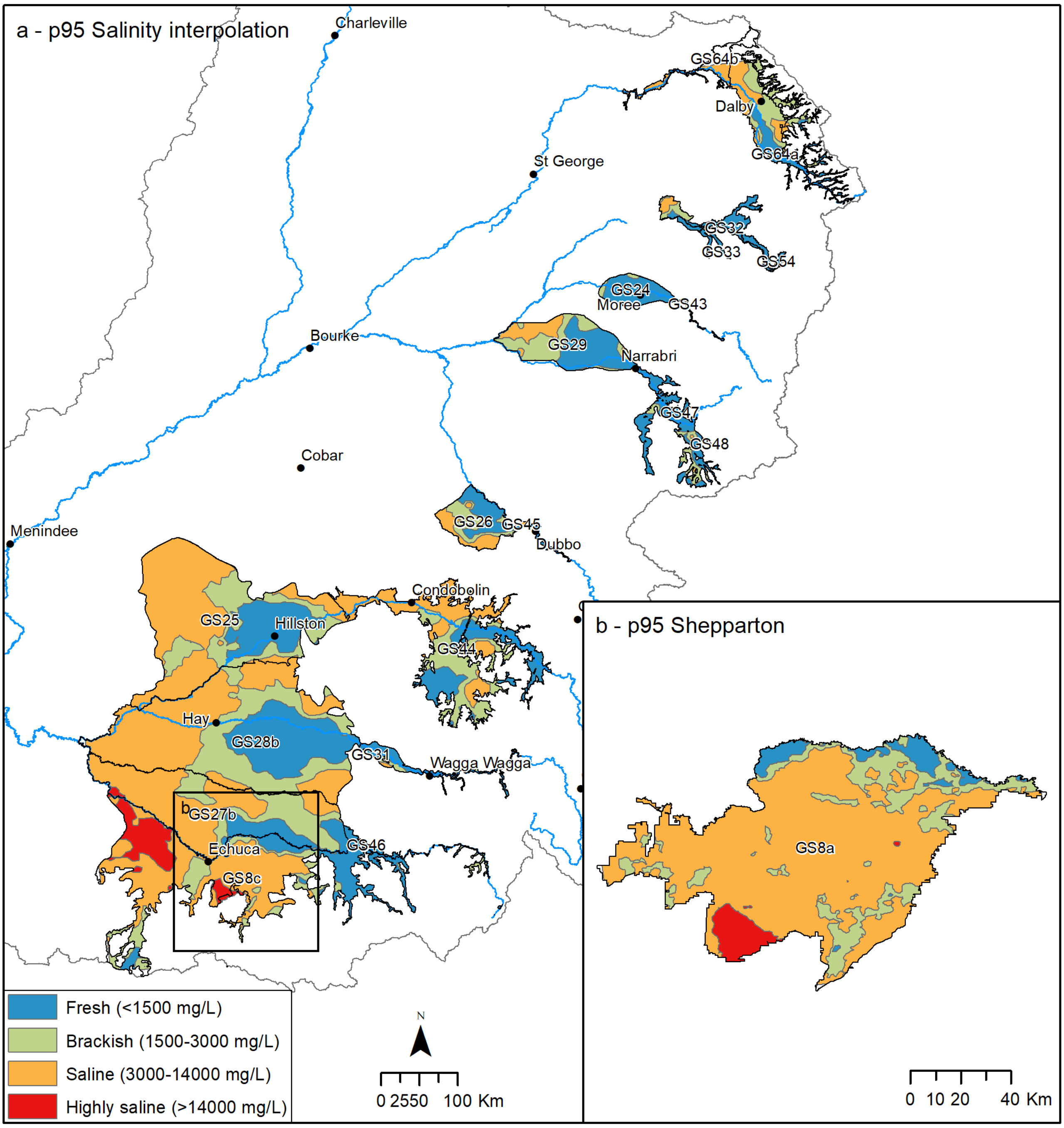

Figure 3 Salinity contours interpolated from 95th percentile observation bore data for (a) the main alluvial SDL resource units, and (b) inset showing the Goulburn-Murray: Shepparton Irrigation Region (SIR) (GS8a) that overlies the Goulburn-Murray: Sedimentary Plain (SP) (GS8c); contours were used for calculation of the groundwater stress index (*iGF*) (from Rojas et al. (2023)).

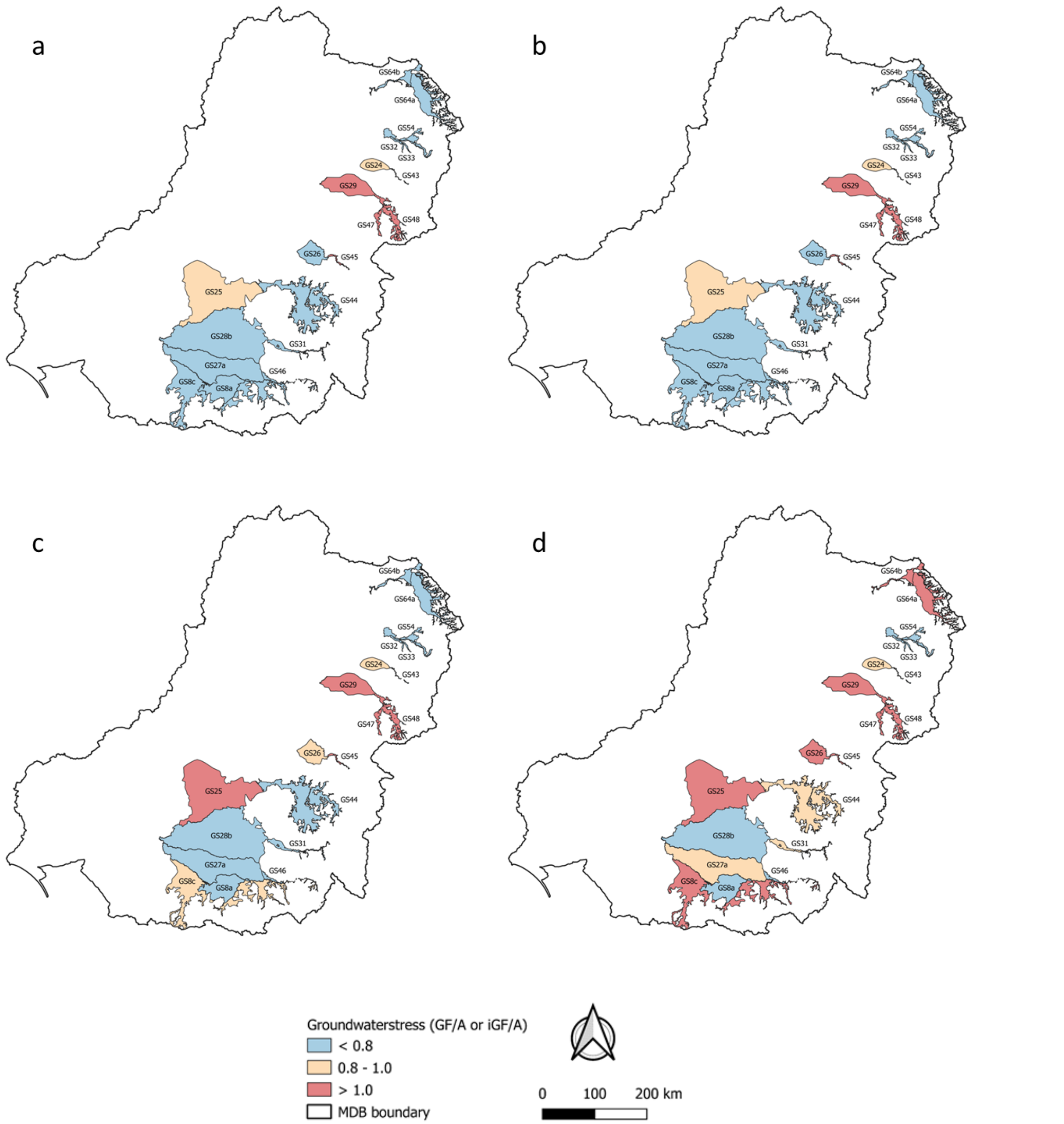

Figure 4 Groundwater stress indices for groundwater SDL resource units considering (a) groundwater use only (*GF/A*) and different salinity classes (*iGF/A*): (b) highly saline, (c) highly saline and saline, and (d) highly saline, saline and brackish as defined by MDBA (2020) (from Rojas et al. (2023)).

When including different salinity class areas in the calculation of the *GF*, we observe important increases in stress levels (*iGF* in Figure 4c and 4d). For example, for groundwater resource units initially identified: Lower Namoi, Upper Macquarie, Upper Namoi (GS29, GS45 and GS47); stress levels increase between 60% and 160%, whereas for Lower Lachlan (GS25), a 3.4-fold increase in stress level is observed. Similarly, when using freshwater areas only in the calculation of groundwater stress, i.e., discounting highly saline, saline and brackish groundwater areas in the alluvial aquifers, other groundwater resource units are identified under stress, namely, Lower Macquarie (GS26); Lower Murrumbidgee Deep (GS28b); Upper Condamine Alluvium (GS64a and GS64b), and Goulburn-Murray Sedimentary Plain (GS8c)—the latter showing the largest (3.4-fold) increase in the stress metric.

Figure 5 shows the scores for development, responsiveness, and numerical relevance using different weighting schemes for the Simpson's diversity index (SDI). These results are similar to Shannon's diversity index, which is not included here. One interesting observation is that changes in *f(GDE)* only affect the development and numerical relevance scores, not the responsiveness score. When the Simpson's diversity index is weighted by the GDE area (D vs DA) or the moderate-to-high potential GDE area (DA vs DAf) to calculate *f(GDE)*, we notice discrepancies in the development score for certain groundwater resource units (e.g. Sedimentary Plain GS8c, Upper Condamine GS64a, GS64b, Lower Gwydir GS24). This is expected since these resource units have less than 8% of the total area defined as GDEs. Similarly, when the diversity index is weighted by the GDE areas of moderate-to-high potential, Lower Lachlan, Sedimentary Plain, Shepparton Irrigation Region and Lower Macquarie (GS25, GS8c, GS8a, and GS26) show the largest fluctuations in the development score. Sensitivities in the numerical relevance score (indicated by symbol size in Figure 5) however are less significant, which suggests that the values are robust.

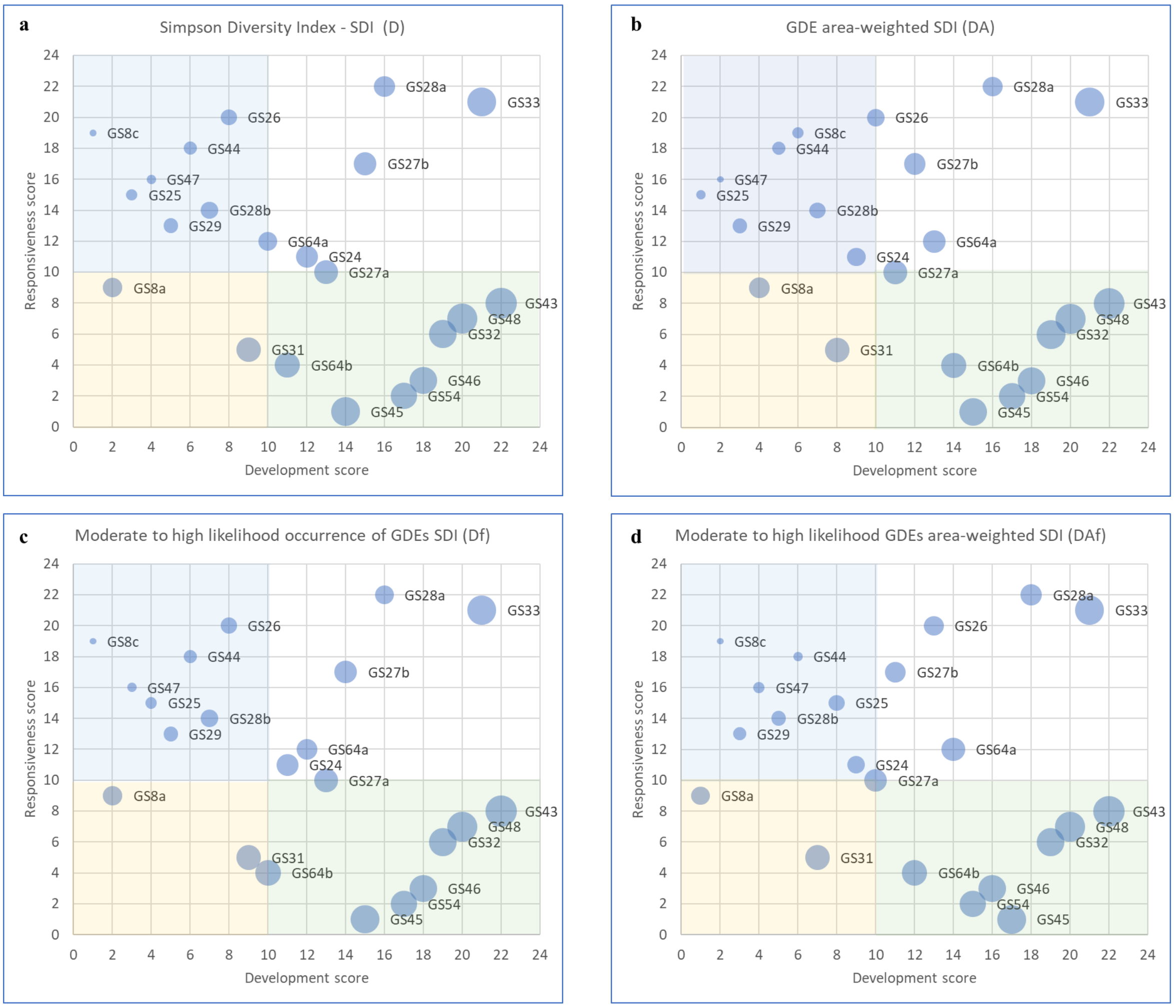

Figure 5 Development, responsiveness and numerical relevance scores for groundwater SDL resource units using (a) Simpson Diversity Index (SDI) (D), (b) area-weighted SDI (DA), (c) SDI using moderate to high GDE potential areas (Df), and (d) area-weighted SDI using moderate-to-high GDE potential areas (DAf). Bubble size reflects numerical relevance (see Appendix A) - small bubbles reflecting high numerical scores and vice versa (from Rojas et al. (2023)).

In Figure 5, the coloured regions in the panels represent the ordination approach. The blue region shows high development and low responsiveness scores, while the green region represents high responsiveness and low development scores. The yellow region reflects high development and high responsiveness scores. To determine the coloured regions of the ordination approach, we established the top 10 (out of 22) groundwater resource units as cut-off values following Barron et al. (2011). The Upper Macquarie (GS45) exhibits a high responsiveness score due to its high *f(R:S)* factor (0.9) and average annual groundwater use (16,643 ML/y) approaching the sustainable diversion limit value of 17,900 ML/y. On the other hand, the Goulburn-Murray: Sedimentary Plain (GS8c) and the Shepparton Irrigation Region (GS8a) show high development scores. However, when the diversity index (D) is weighted by GDE area (DA), Lower Lachlan (GS25) ranks first, followed by Upper Namoi (GS47). This is because of the high ratio of groundwater extraction of Lower Lachlan GS25 and Upper Namoi GS47 compared to the largest groundwater extraction across all groundwater resource units and the changes in *f(GDE)* observed in GS8a and GS8c when weighting the diversity index by GDE area. It is worth noting that the groundwater resource units located in the blue region are the ones that hold the highest numerical relevance score, as indicated by their bubble size. In contrast, those found in the green region with high responsiveness scores have little impact on the numerical relevance score. Therefore, it is the development score that significantly influences the numerical relevance score. However, it is important to mention that some groundwater resource units with a high numerical relevance score (small bubble size) may not necessarily fall within the yellow area defined by the ordination approach.

Based on the ordination approach, two groundwater resource units (Shepparton Irrigation Region and Mid-Murrumbidgee Alluvium) consistently displayed high development and responsiveness scores across various weighting schemes as demonstrated in Figure 5. In the case of Shepparton Irrigation Region (GS8a), this is primarily due to the ratio between SDL_{GS8a} (244,100 ML/y) and SDL_{Max} (GS28b, 273,600 ML/y) used in the calculation of the development score (equation 1). This ratio signifies the proportion of the sustainable exploitable resource in Shepparton Irrigation Region compared to the largest unit in the dataset (Lower Murrumbidgee Deep Alluvium GS28b). It is important to note that the average groundwater use measured in Shepparton Irrigation Region from 2012 to 2019 represents only 23% of its sustainable diversion limit (SDL_{GS8a} = 244,100 ML/y). On the other hand, for Mid-Murrumbidgee, the high scores are mainly attributed to the ratio between the metered groundwater use from 2012 to 2019 (38,957 ML/y) and the SDL (53,500 ML/y) used in computing the responsiveness score (equation 2), along with a moderate R:S ratio.

2.4 Aspects of resilience, stress and sustainability of alluvial aquifers of the MDB

To analyse the resilience, stress, and sustainability of groundwater, standardized indicators are used as proxies. Figure 6 summarises the standardised groundwater-based indicators used as proxies for analysing groundwater resilience, stress and sustainability aspects. Results show eleven groundwater resource units where resilience, stress or sustainability issues have been identified: Lower Gwydir Alluvium (GS24), Lower Lachlan Alluvium (GS25), Lower Murrumbidgee Deep Alluvium (GS28b), Lower Namoi Alluvium (GS29), Mid-Murrumbidgee Alluvium (GS31), Upper Lachlan Alluvium (GS44), Upper Macquarie Alluvium (GS45), Upper Namoi Alluvium (GS47), Upper Condamine Alluvium (CCA) (GS64a), Goulburn-Murray: Shepparton Irrigation Region (GS8a) and Goulburn-Murray: Sedimentary Plain (GS8c). Out of these groundwater resource units, evidence indicates that stress, resilience and potential sustainability issues are simultaneously identified for the Namoi alluvial aquifer (comprising GS29 and GS47). In contrast, the Mid-Murrumbidgee alluvial aquifer (GS31) shows resilience and sustainability issues. For the case of the Upper Condamine Alluvium (GS64a), Lower Murrumbidgee Deep (GS28b) as well as the Goulburn-Murray: Sedimentary Plain (GS8c), evidence suggests groundwater management units experience resilience issues due to declining groundwater levels and high depletion rates, potential stress issues when considering salinity levels in groundwater stress calculations, and potential sustainability issues when presence and diversity of GDEs are considered. Upper Macquarie (GS45) shows stress issues mainly driven by the reported contribution from groundwater to streamflow (MDBA, 2020). In contrast, Upper Lachlan (GS44) shows resilience issues driven by the number of wells showing statistically significant declining trends and high depletion rates, and potential sustainability issues driven by the aquifer development score. A similar pattern is observed for GS8a but with strong evidence from the development score (and ordination approach), indicating sustainability issues. Lower Gwydir (GS24) and Lower Lachlan (GS25) show above-average values for all indicators (across all resource units) used as proxies to analyse resilience, stress and sustainability. Except for lower Lachlan (GS25) stress issues when considering groundwater salinity, all other indicators are similar for these two groundwater resource units, thus indicating no clear evidence of specific resilience, stress or sustainability issues.

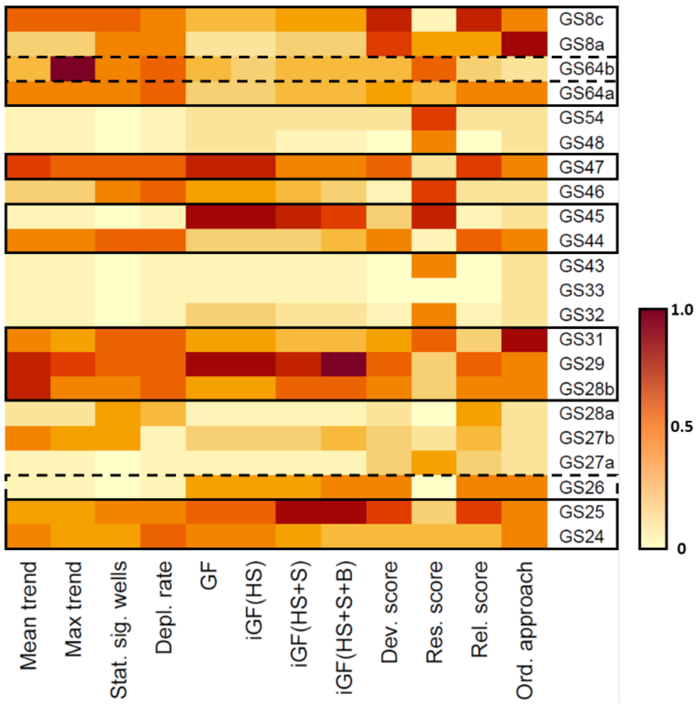

Figure 6 Heatmap representing standardised groundwater indicators of resilience, stress and sustainability for groundwater resource units used to manage the main alluvial aquifer systems in the MDB. iGF(HS): highly saline areas; iGF(HS+S): highly saline and saline areas; iGF(HS+S+B): highly saline, saline and brackish areas. Solid line boxes identify resource units where normalised groundwater indicators for resilience, stress or sustainability are above average. Dashed line boxes identify two resource units where groundwater indicators indicate emergent issues (from Rojas et al. (2023)).

Similarly, emerging stress and sustainability issues have been identified for Lower Macquarie Alluvium (GS26) when groundwater salinity and the occurrence and diversity of GDEs are considered. In contrast, for the Upper Condamine Alluvium (Tributaries) (GS64b), potential resilience issues have been identified (localised highest maximum trend values across resource units).

3 Cluster analysis of groundwater level trends and causal attribution

This section pertains to a research article that is currently being prepared for submission to a peer-reviewed journal. Its focus is on examining the spatial and temporal patterns of groundwater levels at the SDL scale in the main alluvial aquifers of the MDB (as shown in Figure 1). The article compares alternative techniques (i.e., hierarchical clustering analysis and unsupervised clustering through self-organising maps), analyses spatial clusters in these trends, and assesses the potential impact of the Millennium Drought on groundwater levels across the main alluvial aquifers. Additionally, it delves into aspects of causal attribution to better understand the driving factors behind these patterns in groundwater levels. The following sections provide a summary of the methods and results presented in this article.

3.1 Scope

For most of the alluvial aquifers of the MDB, a dominant decreasing trend was observed for the groundwater levels, whereas over a reduced number of observation bores an increasing trend was probably reflecting local conditions associated to aquifer confinement or localised recharge due to flooding or irrigation (Figure 7). These dominant trends are more pronounced in specific groundwater resource units. Similarly, the number of observed DTW records to build these trends varies substantially among resource units and as such the confidence in the estimated trends. For example, Lower Murray Deep Alluvium (GS27b) has only four observation bores (Table 2) fulfilling the selection data criteria, i.e., at least two record per year for a 40-year period, which is reflected in the reduced number of records to fit the trend in Figure 7.

We improved the understanding on these groundwater level trends by performing cluster analysis to untangle the dominant spatial and temporal patterns observed in these trends. Important questions addressed were: What are the dominant patterns in groundwater level trends? How robust are these patterns to different clustering techniques? What is the performance of these clustering techniques? Is there a spatial configuration for these patterns? What is the impact of the Millennium Drought on these patterns?

In this section we discuss and apply two clustering techniques to analyse the dominant patterns in the groundwater level trends: hierarchical and unsupervised clustering. The latter is implemented through the self-organising map (SOM) algorithm (Kohonen, 1990). Both clustering techniques are further compared in terms of numerical performance, and the main dominant clusters in the trends are identified. Dominant clusters are further analysed in spatial terms and the impact of the Millennium Drought on the dominant patterns is analysed.

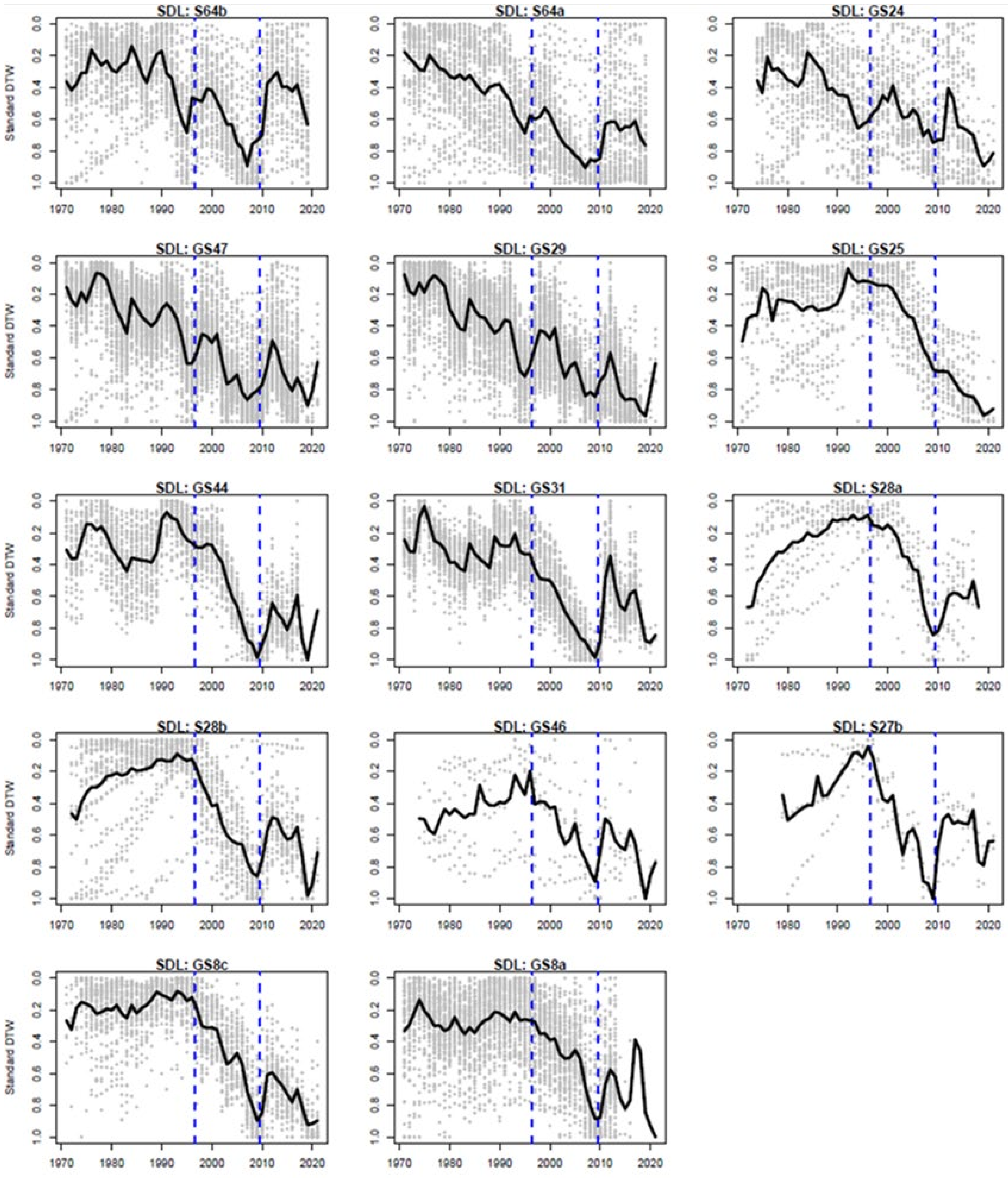

Figure 7 Standardized groundwater level trends for each groundwater SDL obtained from 910 observation bores. Light grey dots represent recorded values for depth to standing water level (DTW).

3.2 Hierarchical clustering

Hierarchical clustering, also called hierarchical cluster analysis (HCA), is an algorithm that seeks to build a hierarchy of groups or clusters so that each cluster is distinctive from other clusters but the elements within the same cluster are broadly similar. The results of hierarchical clustering can be presented as a dendrogram, which is a diagram with a tree structure representing the hierarchical relationship between elements (Nielsen, 2016). To determine which cluster, the individual element belongs to, a metric is needed to measure the distance between this element and other elements and clusters. The Euclidean distance is the most popular choice and is used in this study (Nielsen, 2016).

Figure 8 is the dendrogram of the depth to standing water level (DTW) with 910 bores used in this study. The six clusters/groups are chosen for this study based on the distances among them and their temporal patterns (Figure 9). A large proportion of the trends in the observation bores fall within two dominant clusters (Clusters 1 and 2).

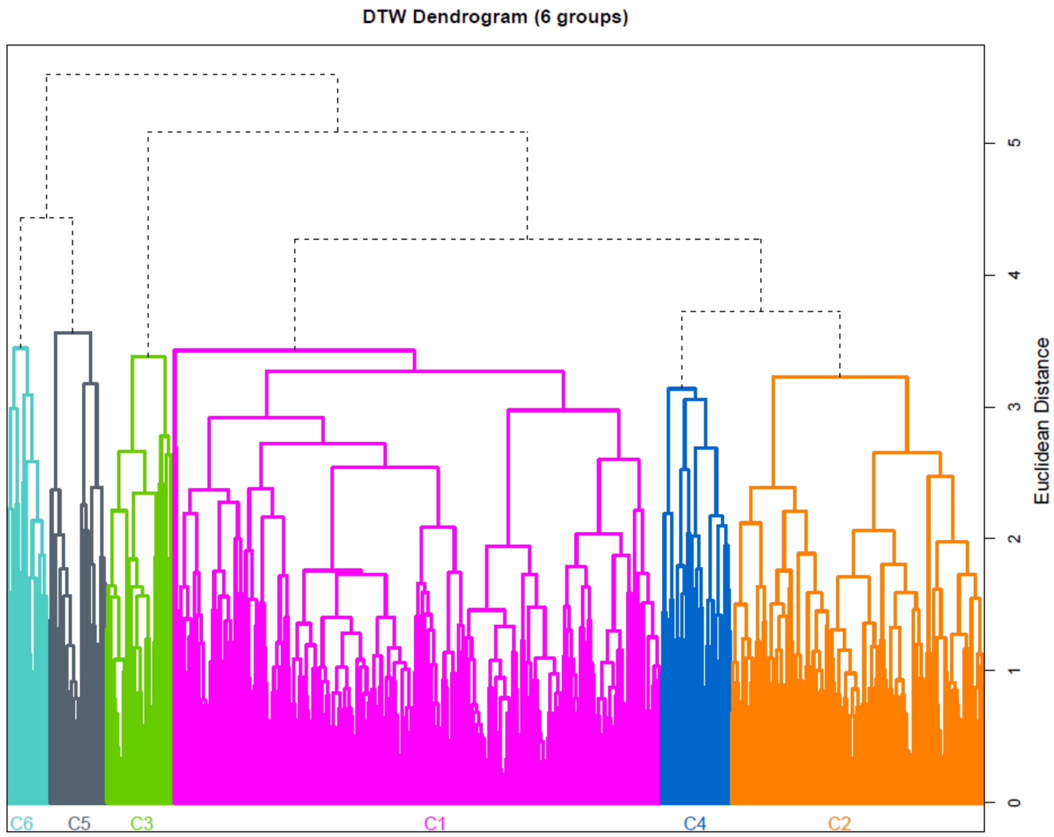

Figure 8 Dendrogram of depth to standing water level (DTW) from 910 bores (6 groups/clusters).

Figure 9 shows the temporal variations of the mean values of the standardized DTW from the six clusters. The vertical blue dashed lines represent the Millennium Drought period in 1997–2009, a severe and prolonged dry period in southeast Australia. The rainfall, streamflow, groundwater level and storage, wetland, lakes and their relationships have changed significantly, before, during and after the Millennium Drought (Fu et al., 2023). Each cluster displays a unique temporal pattern of DTW: 1) There are 454 (about 50%) of groundwater bores in Cluster 1 (C1 in Figure 8), which show a continuous decreasing of groundwater level during 1971–2019, i.e., before and during the Millennium Drought periods (Figure 9). However, the groundwater level is relatively stable after the drought. The 2011–2012 wet years can also be observed; 2) There are 236 (about 26%) of groundwater bores in Cluster 2 (C2 in Figure 8), which show a stable groundwater level in 1971–1996 before drought period, but a decreasing trend during and after the drought periods (Figure 9). The 2011–2012 wet years can also be observed in this cluster; 3) There are 62 (about 7%) of groundwater bores in Cluster 3 (C3 in Figure 8), which show a significant decreasing trend of groundwater level in 1971–1996 before drought period, but relatively stable during and after the drought periods; 4) There are 65 (about 7%) of groundwater bores in Cluster 4 (C4 in Figure 8), which show an overall decreasing trend of groundwater level for the entire study period. However, it shows the greatest fluctuation, implying the sensitivity of groundwater level to rainfall anomaly (Figure 9). The 2011–2012 wet years lead to the biggest jump of groundwater level in this cluster; 5) There are 53 (about 6%) groundwater bores in Cluster 5 (C5 in Figure 8), which show an increasing trend of groundwater level in 1971–1996 before the drought period, but a decreasing trend during and after the drought periods (Figure 9). The increasing trend in 1971–1996 should be the result of human activity, such as irrigation, and the significant decreasing trend during the drought period should be a result of drought events; 6) There are 40 (about 4%) of groundwater bores in Cluster 6 (C6 in Figure 8), which show the similar increasing trend of groundwater level as Cluster 5, but relatively stable of groundwater level during and after the drought (Figure 9). The underlying physical processes could be a mixed impact of human activity and climate change, i.e., the effects of dry climate are offset by human activity.

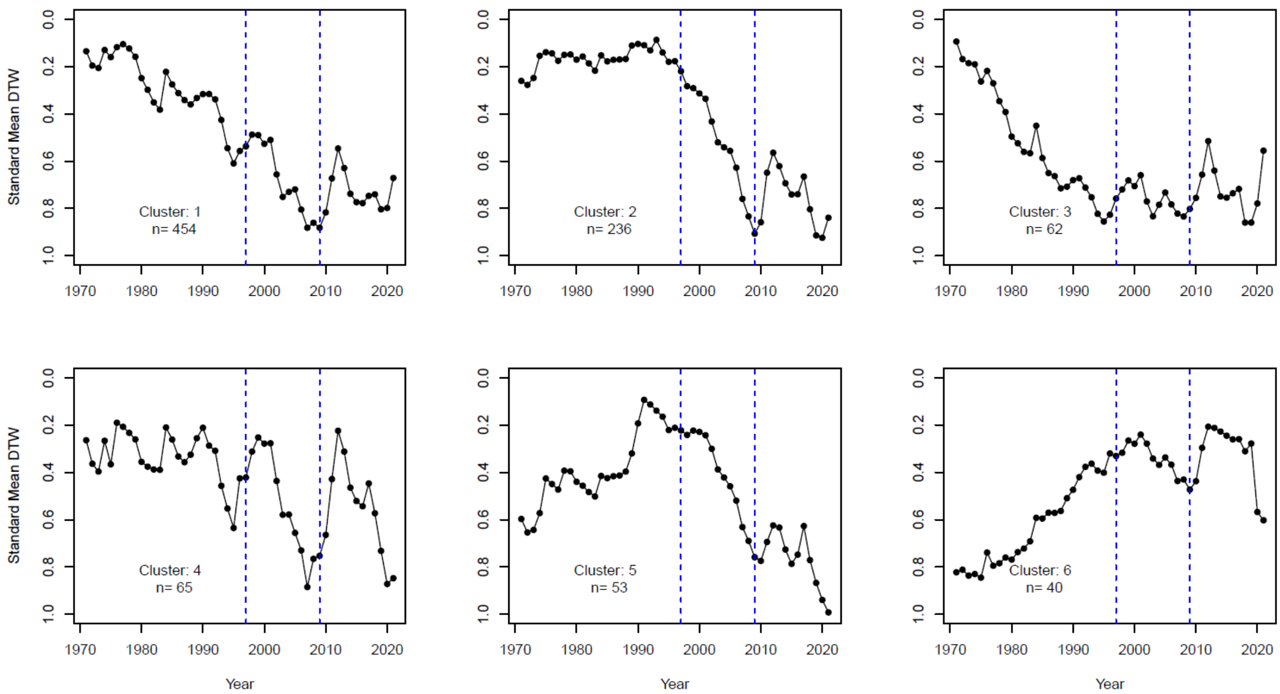

Figure 9 Time series of mean standardized DTW from six clusters (vertical blue dash lines represent the Millennium Drought perios 1997–2009).

3.3 Unsupervised clustering – Self Organising Maps (SOMs)

The self-organising map algorithm is from the family of unsupervised neural networks, used for clustering, dimension reduction and visualisation. Being 'unsupervised' means it is able to determine relationships in the data that are not provided as input and can therefore extract patterns in the data that are not known beforehand. The SOM works by placing a mesh of interconnected nodes over a high-dimensional data cloud and through an iterative process refines the placement of the nodes to best represent the shape and density of the data, whilst maintaining a connection between neighbouring nodes. This process determines the most prevalent patterns that are present in the dataset. After the training process is complete, the data items are each matched to the nearest node of the map, creating clusters of data with similar patterns. For more information on the SOM algorithm, see Clark (2022) and Kohonen (1990).

As with the hierarchical clustering above, here the observation bores are clustered based on annual average depth to standing groundwater levels (DTW). Before clustering, the water levels are scaled into the range [0,1] to enable comparison between groundwater level variations that occur on different scales.

The results of the self-organising map are shown in Figure 10. Levels have been inverted (Water level = 1 - Depth to Groundwater) for intuitive interpretation - a declining line on the plot indicates a declining groundwater level. The number of bores in the data set which are best represented by each pattern is indicated in the lower left of each subplot.

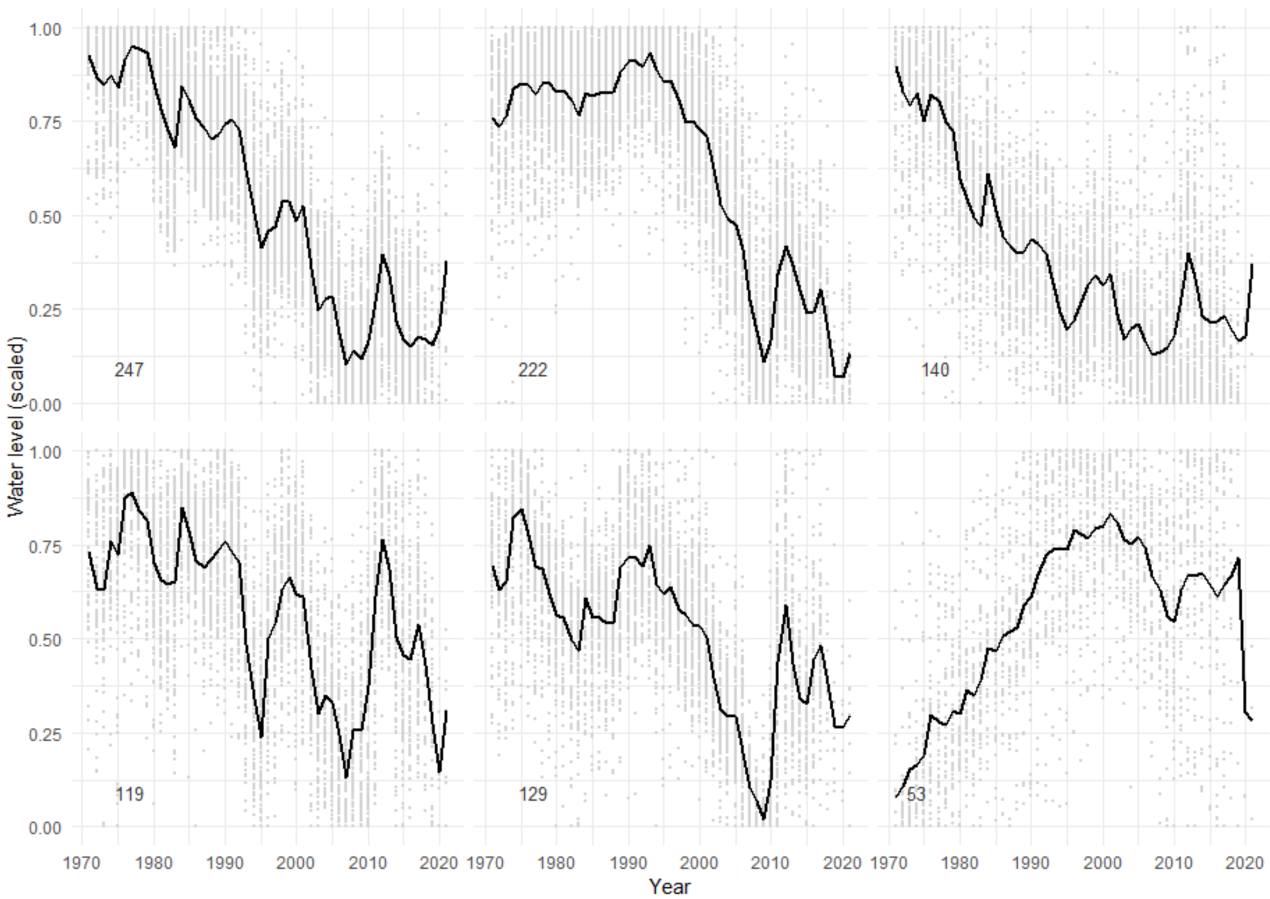

Figure 10 Clusters of groundwater level time series as found with the self-organising map algorithm. The main pattern of each cluster is shown (black line), along with the measurements from bores matched to each pattern (light grey points). The number of bores that best match each pattern is noted for each subplot.

3.4 Comparison and performance of hierarchical versus SOM clustering

Comparing the clustering results of the hierarchical and SOM methods (considering clusters to be numbered 1-3 from left to right on the top row and 4-6 on the lower row), the patterns from both methods correspond well for all clusters with the exception of cluster 5. The number of time series (observation bores) that best match each pattern differs between methods, with about half of the time series that are attributed to Cluster 1 with the hierarchical clustering method spread between Clusters 3, 4, and 5 with the SOM. The number of time series in Clusters 2 and 6 are almost the same for both clustering methods.

Figure 11 shows the spatial comparison of the patterns obtained from hierarchical clustering and SOM. In terms of the mean square error (MSE) both clustering techniques show similar numerical performance. Overall, the six dominant clusters in groundwater level trends are correctly identified by both techniques. Two areas of discrepancy arise in the upper Condamine Tributaries and Mid-Murrumbidgee. In the former, clusters identified correspond to Cluster 4 (SOM) and Cluster 1 (HC). Both clusters are similar with the cluster identified by SOM showing a higher range in the representative times series. For Mid-Murrumbidgee the clustered patterns are similar and only differences in the stable trend prior to the pronounced declining trend are observed, e.g., Cluster 5 (SOM) vs Cluster 2 (HC).

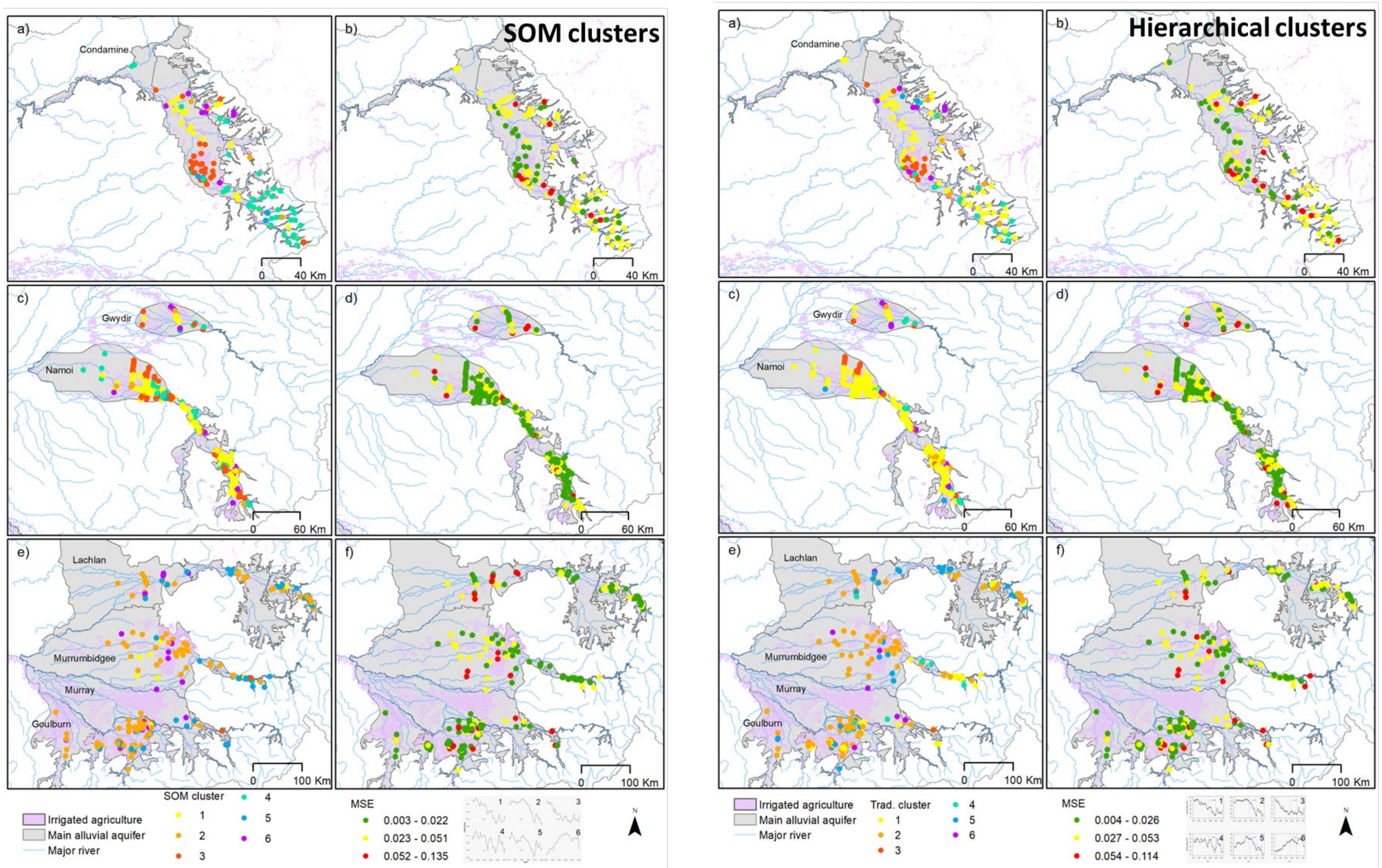

Figure 11 Comparison of Hierarchical and SOM clustering techniques. Panels a, c and e, cluster groups. Panels b, d and f, mean square error (MSE)

3.5 Geographical analysis of clustering results

A geographic analysis of the SOM clustering results is shown in Figure 12. Bores are coloured by cluster as indicated in the legend.

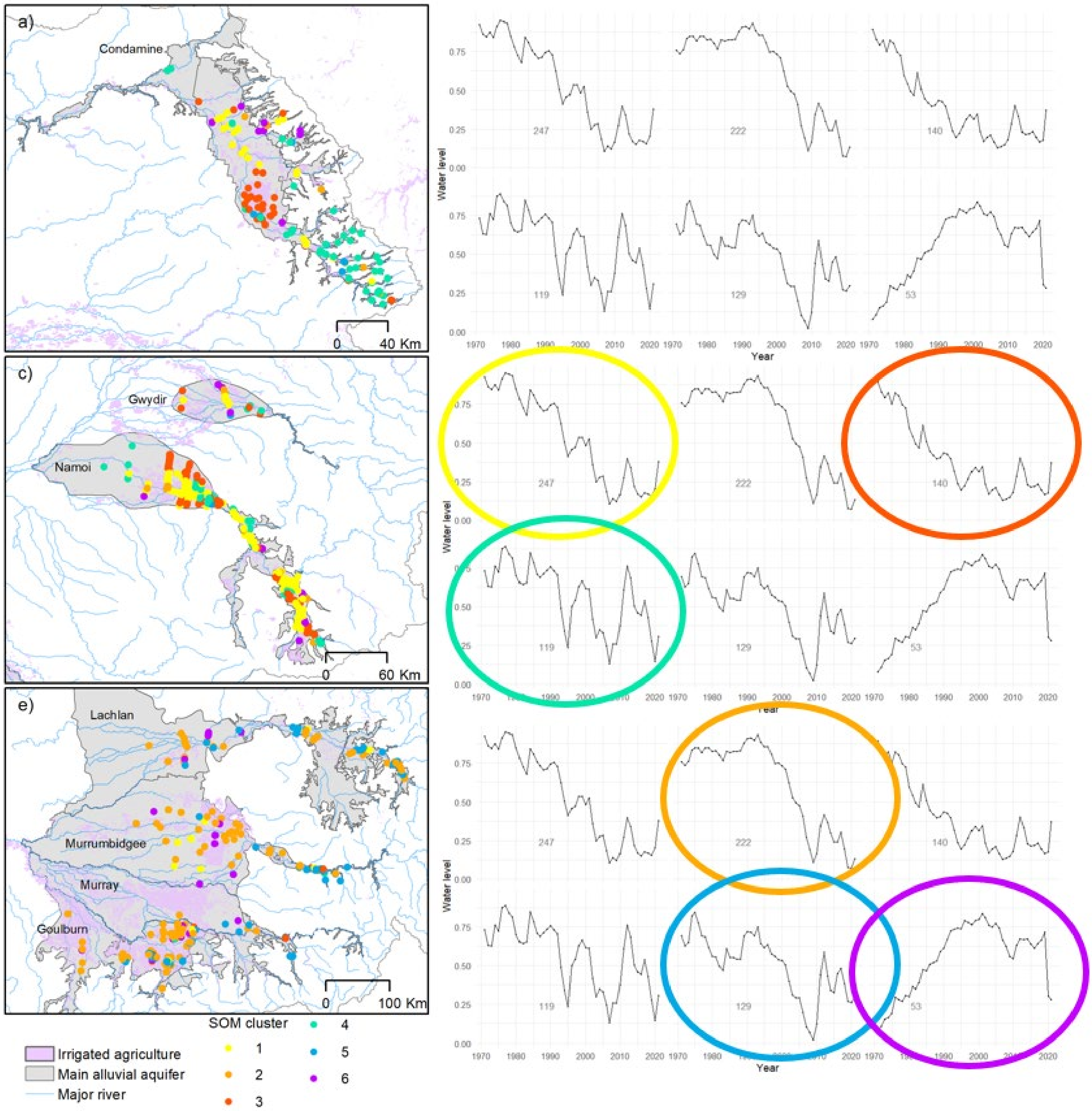

Figure 12 Geographic representation of SOM clustering.

It can be seen that the region shown in the upper panel (a) Condamine) contains a mixture of all patterns; the middle panel (c) Namoi, Gwydir) has mostly yellow and red bores (relatively constant decline before and during drought, evening out post-drought), with some turquoise - the turquoise pattern is similar to the yellow and red but shows better recovery between drawdown events; and the region in the lower panel (e) Lachlan, Murrumbidgee, Murray, Goulburn) is dominated by orange (stable pre-drought followed by a steep decline during the Millennium Drought) with some blues (steep decline but more recovery) and purples (increasing before and immediately after the drought).

The geographic distributions of hierarchical clustering results are generally consistent with those of the SOM clustering results (Figure 11). However, one of the significant differences is that Cluster 1 (C1 in Figure 8 and Figure 9) includes 454 out of 910 of groundwater bores (about 50%) from hierarchical clustering, but only 247 out of 910 bore (27%) based on SOM clustering (Figure 10), indicating that Cluster 1 has a wider spatial distribution for hierarchical clustering results (Figure 11).

3.6 Temporal analysis and impact of the Millennium Drought (MD) on clustering results

As this data set contains groundwater level measurements from before, during and after the Millennium Drought, further analysis is conducted here to determine whether areas with similar groundwater patterns before and during the drought continued to behave similarly after the drought. The time series are split into three periods corresponding to: before (1971-1996), during (1997-2009) and after (2010-2021) the Millennium Drought (Fu et al., 2023).

However, we cannot use all 910 bores for this analysis, as the data filtering criterion (at least two records for a 40-year period) applies to the entire study period 1971–2021, which could potentially lead to a very small sample size for one period. For example, all 11 missing years might be located at the post-drought 2010–2021 period, resulting in only 1 data point available for the groundwater level time series at this bore, and accordingly a meaningless trend magnitude.

A sub-set of 661 among 910 bore data is selected by requiring at least 70% data points of groundwater level time series at each of three time periods, i.e., before, during and after the Millennium Drought.

Figure 13 shows the cumulative distribution function of trend magnitude of depth to standing water level (DTW) in these three periods. The magnitude value indicates the rate of change of the groundwater level over time. Because it is based on depth to standing water level measurements, a positive magnitude indicates a decline in groundwater level, i.e., groundwater level becoming deeper with time.

Over this sub-set of bores, it is evident on Figure 13 that the trend magnitudes are the largest (indicating a steeper decline in groundwater level) during the Millennium Drought period due to the dry climate. In contrast, trend magnitudes before the drought are the smallest because of wet climate, and the magnitudes after the drought generally fall into the middle, except the negative trend magnitudes. The negative trend magnitudes after drought period at 20–25% groundwater bore locations imply the recovery of groundwater level from dry period with wet climate condition. The rest 75–80% bores still show a decreasing of groundwater levels, but their magnitudes are smaller than those observed during the drought period.

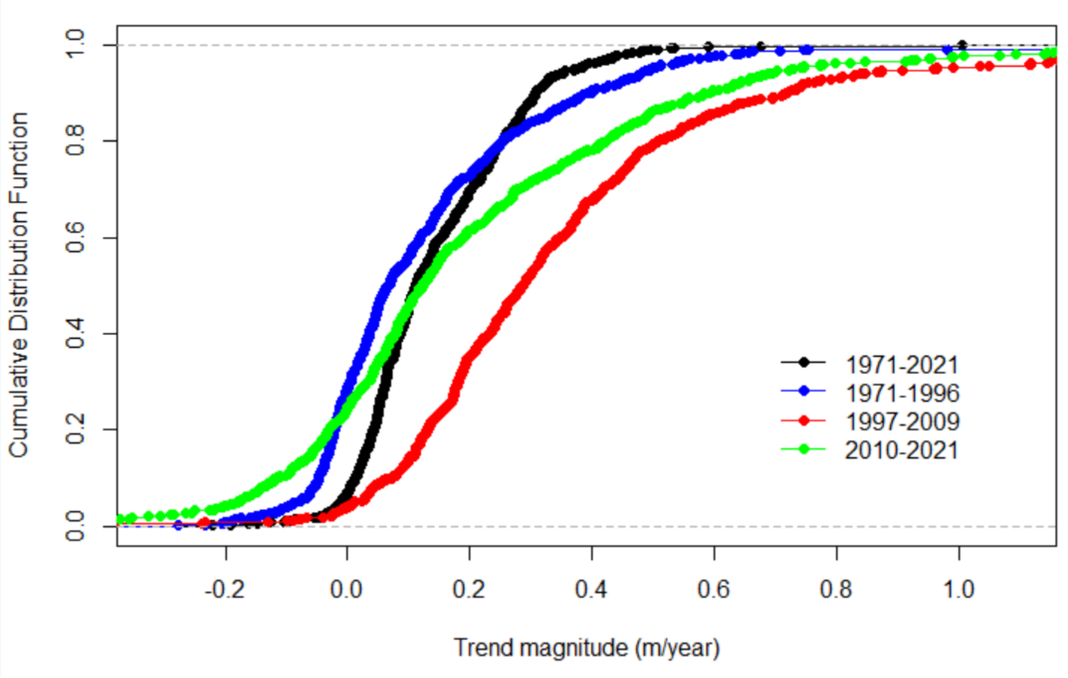

Figure 13 Slopes of DTW time series separated into 3 segments: before MD 1971-1996 (dark blue), MD 1997-2009 (red), after MD 2010-2021 (green), and entire time series 1971-2021 (black). Positive slopes mean the groundwater level is decreasing over time. Each time series has a dot of each colour representing its slope in each of the 3 time periods. Observation bores are arranged along the x-axis by slope of the 2010-2017 segment.

The SOM in Section 3.3 was based on clustering the groundwater time series to determine similarities that exist over the entire time period (1971-2021). However, the large variation in groundwater level time series gradients that has become evident in the third period (after the Millennium Drought) may provide insightful information into recent regional groundwater behaviour – observation bores that were behaving similarly before and during the drought may have different post-drought responses.

Here, a new SOM is created in which the set of time series are first clustered based on before- and during-drought patterns, and these clusters are then refined by post-drought information. The three main patterns identified in the data before and during the drought by this SOM are shown in Figure 14. Note that there are now 3 main patterns identified rather than the 6 identified in the previous section as the post-drought period is not being considered here. On Figure 14, the three main patterns are characterised by: groundwater levels remaining steady before the drought followed by a swift decline during the drought (on the left), a constant decline before and during the drought (centre), and a general increase in groundwater levels until the drought followed by a decline (on the right).

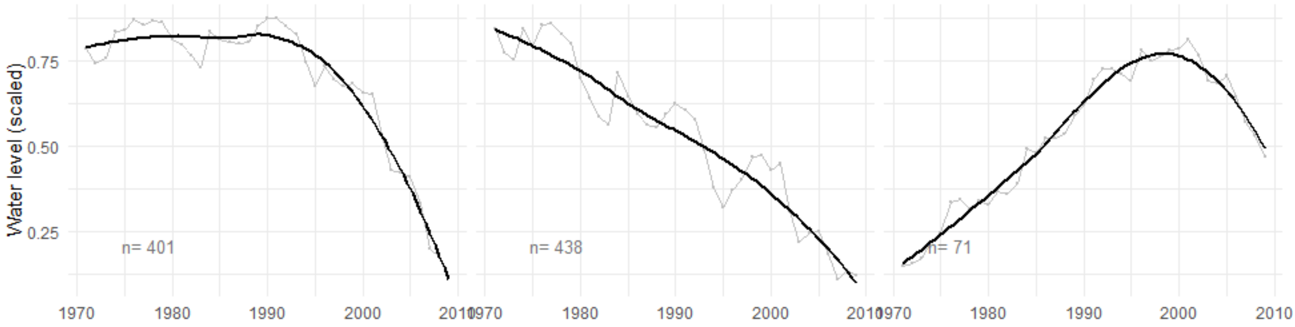

Figure 14 Three main patterns in groundwater levels before and during the Millennium Drought (1971-2009) as found by the SOM algorithm. The number of time series that match each pattern is denoted in the lower left of each plot.

These groundwater level patterns before and during the drought can now be refined by information from after the drought. The 401 bores from the first cluster of Figure 14 (with groundwater levels steady before the drought and declining during the drought) are further clustered in Figure 15 based on the post-drought measurements. Four patterns of post-drought behaviour are observed, all of which have some degree of increased groundwater level immediately following the drought (Figure 15a). After this initial post-drought increase, the behaviour diversifies into further increase, steadying or declining. On Figure 15b, the origins of these patterns are aligned for comparison of the potential groundwater level paths for these bores that had similar before and during drought behaviour.

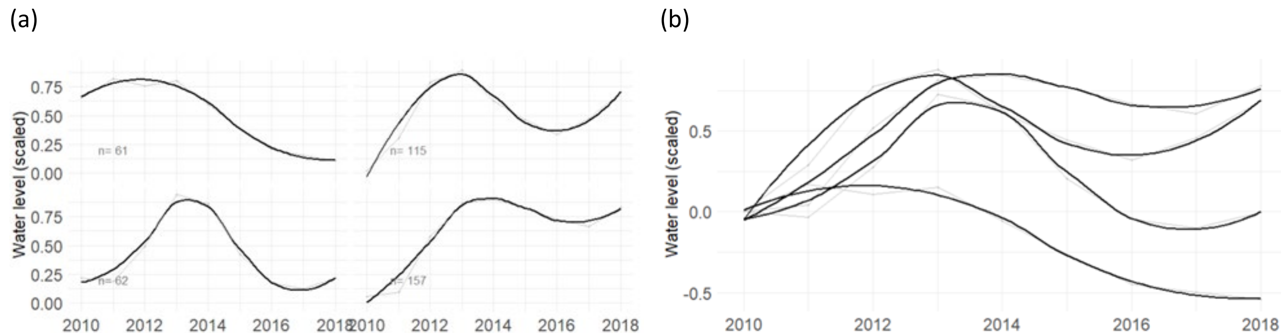

Figure 15 Prevalent patterns of post-drought behaviour (2010-2018) in groundwater time series that were steady and then declining before and during the Millennium Drought (first cluster of Figure 14).

3.7 Causal attribution

Understanding the main factors driving groundwater level changes in these aquifers will help to focus specific efforts for mitigating groundwater level changes. Different drivers will affect groundwater levels differently in each region. For example, groundwater extractions may be strongly influencing groundwater depletion in some resource units, whereas other resource units may be more affected by changes in rainfall and PET. In order to understand which factors may have the greatest effect in each groundwater SDL, a causal attribution analysis will be performed.

3.7.1 Method

The first step in the causal attribution process is to represent the system in terms of a response to predictor variables. In this system, the predictors include annual rainfall (current year and previous year), PET, groundwater use (extractions), and the number of new production/extraction bores. Each groundwater SDL has a single set of predictors (i.e., one value of rainfall/year per SDL). The predictors are shown in Figure 16, with values scaled into the range [0,1] by SDL to facilitate comparisons between systems at dissimilar scales. The system response variable is 'annual change in average groundwater level' at each bore, with each SDL having multiple groundwater measurement bores. Groundwater level measurements have been scaled to the range [0,1] by bore.

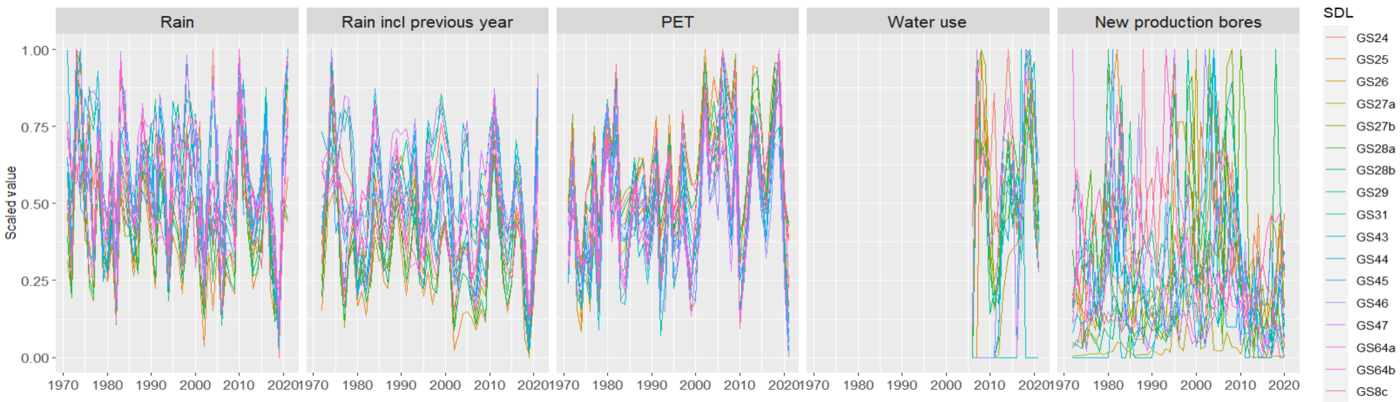

Figure 16 Potential predictors of changes in groundwater levels. This data set has one annual value per predictor for each SDL. The groundwater use data begins in 2006.

Correlations between the system response and each predictor variable give clues to causality. Figure 17 shows scatterplots of the change in measured groundwater level corresponding to each predictor measurement. Smoothers have been added to indicate trend by SDL for the change in groundwater level with respect to each predictor. It can be seen that increasing rain generally corresponds to increasing groundwater levels whereas increasing PET and groundwater use relate to decreasing groundwater levels, though not monotonically. There are noticeably fewer groundwater use data points than other predictors, as the data available for this variable begins in 2006.

A closer look at correlations between predictors and response variables is provided in Figure 18 for two of the resource units (Lower Namoi GS29: magenta, and Upper Lachlan GS44: blue). Density plots and scatterplots of the relationships can be compared for the two resource units. The second row indicates correlations between each predictor variable and the change in groundwater level (labelled 'GWL_delta'). The 'rain_comb' variable, which combines each year's rainfall with the previous year's rainfall, shows a higher correlation with change in groundwater level than the current year's rainfall alone ('rain'). Therefore the 'rain_comb' variable will be used in the remainder of this analysis. For these two resource units, it is apparent that anthropogenic influences on the system appear more strongly through the 'groundwater use' variable for Lower Namoi GS29 whereas the number of new production bores ('prodbore_delta') is more strongly correlated with groundwater levels in Upper Lachlan GS44. The prodbore_delta variable is the cumulative number of new production bores drilled each year within the resource unit based on drilled dates in the NGIS database.

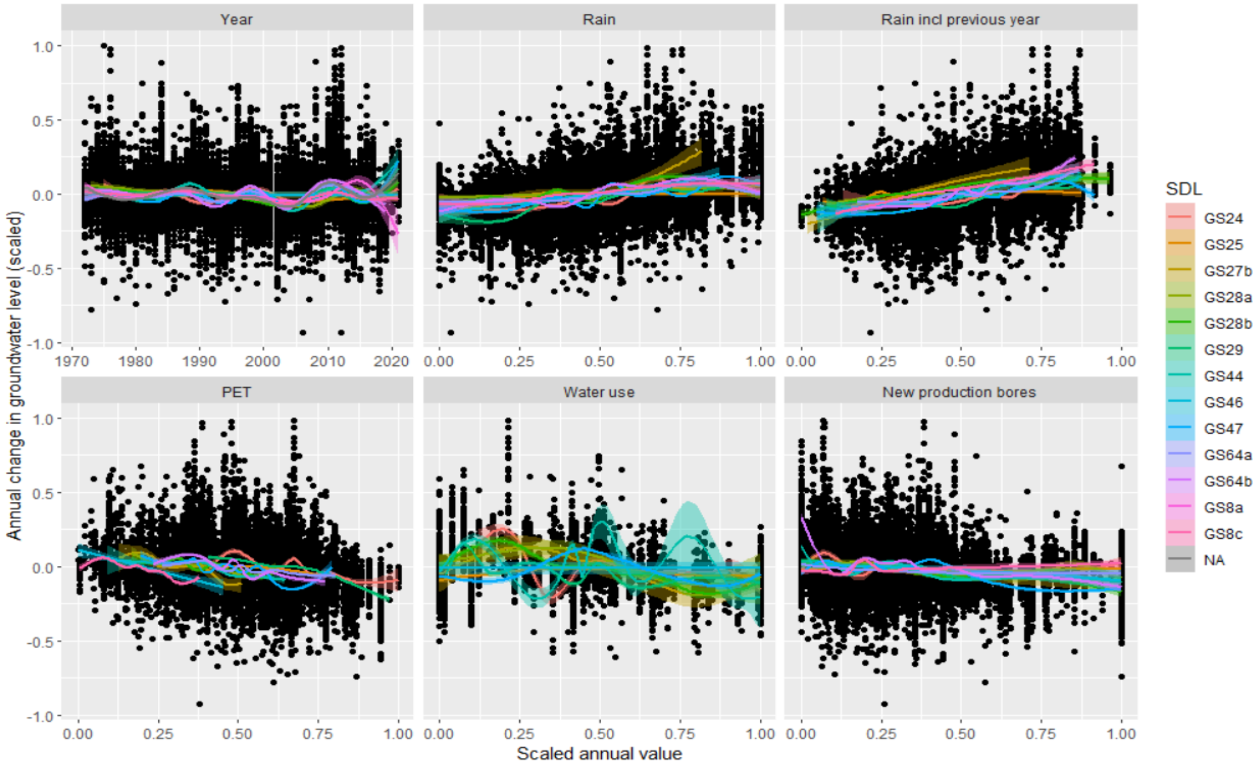

Figure 17 Scatterplots of changes in groundwater levels corresponding to the range of measured predictors. Smoothers (with shaded 95% confidence intervals) indicate general trends by SDL.

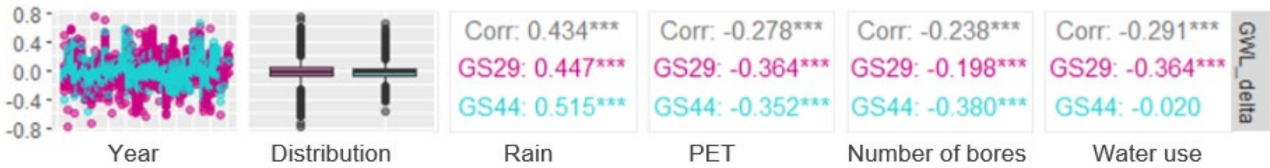

Figure 18 Correlation of changes in groundwater level (‘GWL_delta’) with predictors for two example SDL’s (Lower Namoi GS29 in purple, Upper Lachlan GS44 in blue). Rainfall shows a positive correlation and potential evapotranspiration a negative correlation for both, whereas groundwater use and the number of production bores negatively impact groundwater levels differently for each SDL

Neural network models are used to model the changes in groundwater levels for the set of predictors. In producing these models, a number of considerations must be made:

- *Predictors to be included:* data begins in the 1970’s for all variables besides groundwater use, which begins during the Millennium Drought (in 2006). Including the groundwater use data in the model would significantly reduce the length of the analysis and therefore the size of the data set available for model training. However, excluding groundwater use data from the model potentially ignores a significant influence on groundwater level changes.
- *Separate models:* should separate models be created on the SDL level, by cluster, by bore, or one for all regions together? Some resource units have groundwater level patterns that

match more than one cluster and it may be an issue to model these different responses with the same SDL-level predictors.

- *Response times*: groundwater use (extractions) should cause an immediate response in groundwater levels but rainfall may have a longer period of influence. The average annual groundwater level value encompasses the entire year but during the beginning of the year this groundwater level is likely responding to climate conditions captured in the previous year's rainfall and PET values.

The second step in the causal attribution analysis is to interrogate the models to determine how the annual changes in groundwater levels depend on each predictor variable. Using the Permutation Feature Importance method [Breiman, 2001], the importance of each variable to predicting the response of the system is indicated by the difference in model performance when the model is run with this variable permuted (randomised or set to zero). One issue with this method is that if two predictors are correlated, both will be deemed unimportant. In this case, it would be best to separate the predictors into 'climate' influences (rain and PET) and 'anthropogenic' influences (groundwater use and number of bores) before using this method. The error gradients at the weights of the neural networks could also be investigated to identify changes in model response with respect to changes in each predictor variable.

3.7.2 Preliminary results

To match the other parts of this report, the preliminary results shown here are on the SDL level. Preliminary results are given for two SDL's (Lower Namoi GS29 and Upper Lachlan GS44). The neural network models used for this analysis are 2-layer multi-layer perceptrons (MLP's). Model settings (hyperparameters) have not been optimised in this preliminary analysis.

Figure 19 shows the modelled annual change in groundwater level (red) over the scaled measurements from all bores in the SDL (blue). As the predictors are provided at an SDL level, only one modelled response per SDL is produced (rather than one per bore). On the left panel, the predictors are year and climate data only (rain and PET) and this data extends back to 1971. On the right panel, anthropogenic data is added, and here the predictors are year, rain, PET, groundwater use and number of new production bores. As the available groundwater use data begins in 2006, so does this model.

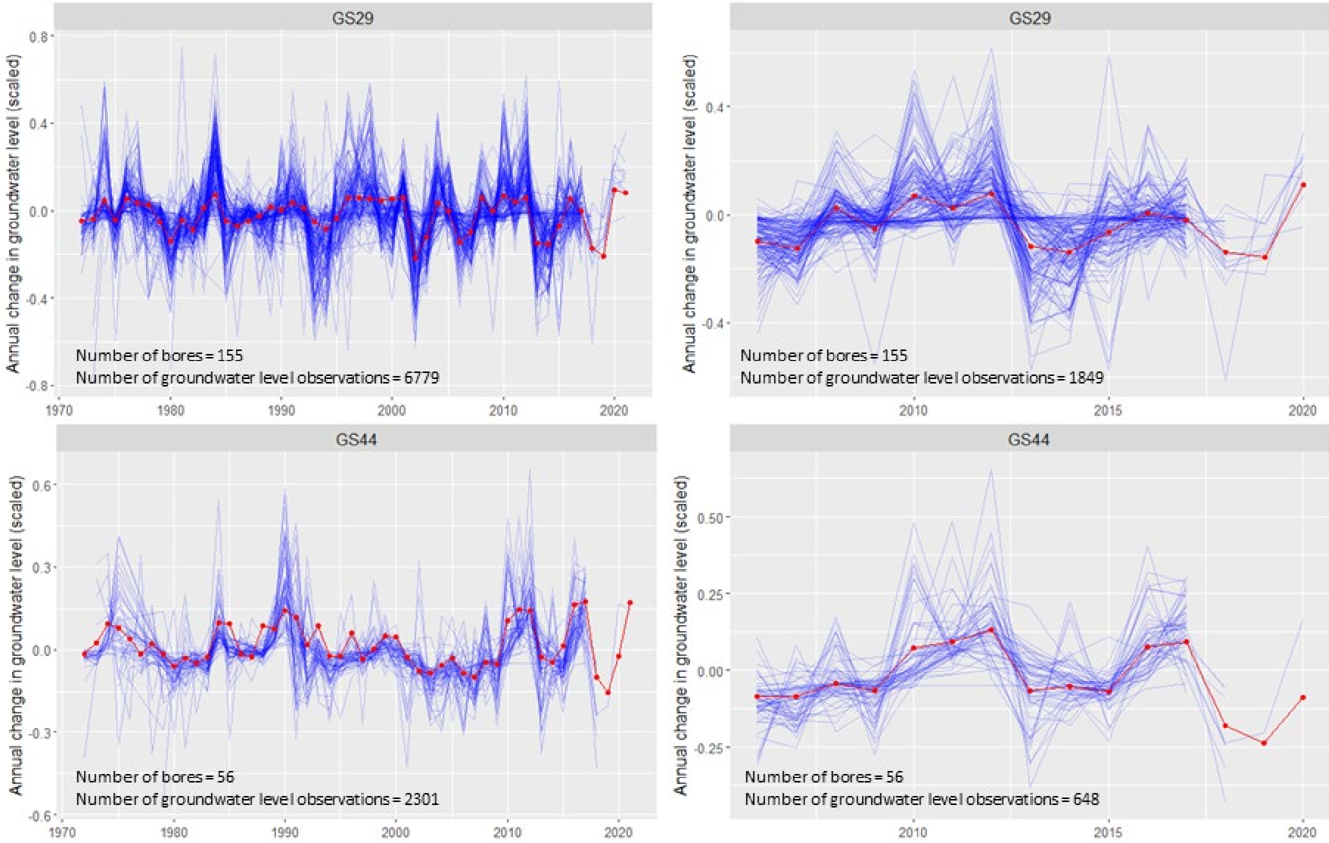

Figure 19 Modelled annual change in groundwater level (red) at the SDL level compared to measured change in groundwater level (blue) at the bore level. Two SDL's are shown (Lower Namoi GS29 and Upper Lachlan GS44). The left panel uses year, rain and PET to predict changes in groundwater levels; the right panel uses year, rain, PET, groundwater use and number of new production bores

Improvements to the current data set, and therefore the modelling results, could include using rain, PET, and groundwater use information on a local basis rather than at the SDLRU level. More granularity is appropriate as climate and groundwater extractions vary within the SDLRU. An increase in the length of the groundwater use data set would also be of benefit.

The above models can be interrogated to determine the impact of each predictor on the response of the system. Figure 20 provides a visualisation of the counterfactual scenario in which no extractions occurred in each SDLRU (groundwater use data set to zero) for the simple models shown in Figure 19. The yellow line indicates the updated prediction for changes in groundwater levels if extractions had not occurred. Without groundwater extractions included in the model, the predicted recharge in groundwater from the other predictors such as rain is increased (as shown by the yellow line higher than the red line). We see the estimated effect of recent groundwater extractions (difference between red and yellow lines) is greater on the model of the Upper Lachlan GS44 than the Lower Namoi GS29. Note that these are sample results only to indicate the type of interrogations that could be made; as the training data for these models currently only extends back to 2006, one prediction is made for the entire SDLRU, and a small set of predictor variables are used, the actual values shown are not as reliable as the fact that one SDLRU appears more affected by groundwater extractions than the other.

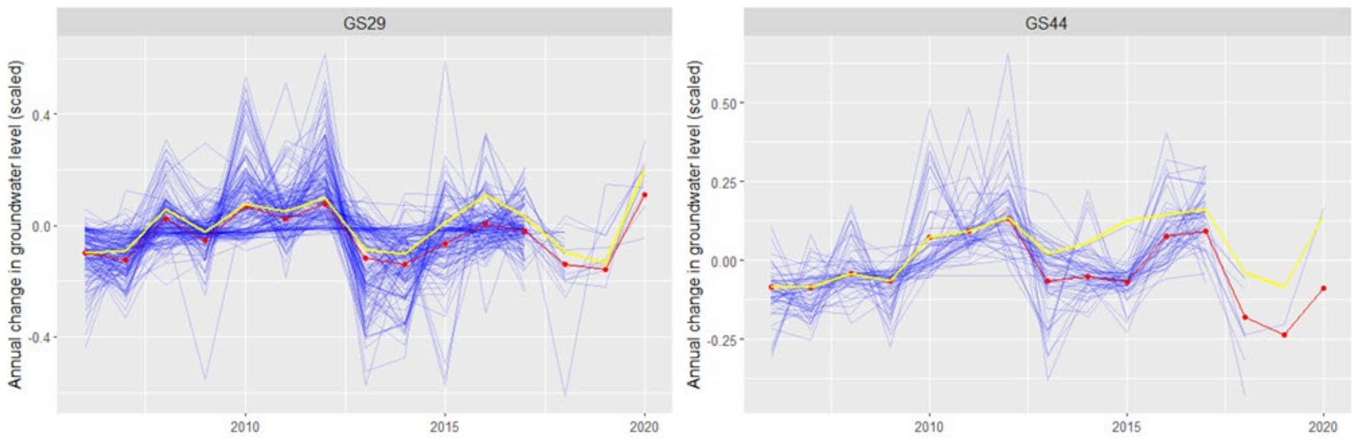

Figure 20 Modelled annual changes in groundwater levels (red) given the historic data, and the hypothetical scenario if no extractions had occurred (yellow). The simulated changes in groundwater levels in Upper Lachlan GS44 are considerably more positive under the no-extraction scenario

Further methods for determining causal attribution might include determining the change in model performance by decade (or other time period). Simulations produced based only on climate data (groundwater use not included in the model) could be expected to show worsening performance over time as increasing groundwater use affects levels. Applying the Permutation Feature Importance method by time period could establish changes in the importance of each predictor in each region as time progresses.

4 Mapping of managed aquifer recharge potential under uncertainty

This section presents a framework for Monte Carlo mapping of MAR potential based on the assessment of aquifer and physiographic features. It builds upon the work by Gonzalez et al. (2020) and the spatial interpolation of the groundwater levels trends obtained from Fu et al. (2022) and discussed in previous sections. By considering groundwater level trends instead of static-in-time groundwater levels, the MAR potential assessment is improved by adding a dynamic aspect to the initial assessment implemented by Gonzalez et al. (2020).

4.1 Scope

The proposed approach will apply a spatial screening analysis methodology that accounts for uncertainty in assessment of managed aquifer recharge (MAR) potential. The study area includes the main alluvial aquifer systems shown in Figure 1. These build on the methods used in an earlier spatial analysis of aquifer storage potential in the MDB (Gonzalez et al., 2020) and a subsequent study that covered other regions around Australia (Page et al., 2021). Gonzalez et al. (2020) focussed on storage potential in unconfined aquifer conditions and used six spatial criteria to indicate where infiltration recharge techniques are feasible (Figure 21).

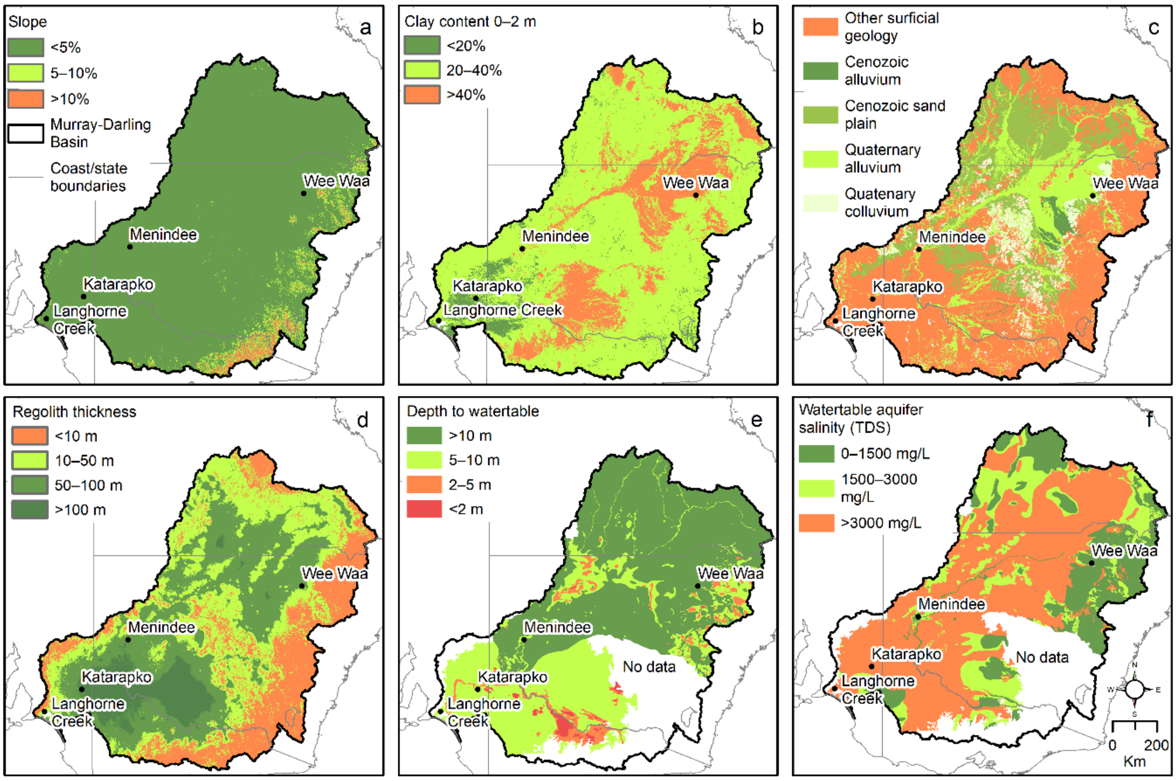

Figure 21 Spatial input parameters for assessment of aquifer storage potential in the Murray–Darling Basin (Gonzalez et al., 2020): **topographic slope (a), soil clay content (b), surficial geology (c), regolith thickness (d), depth to water table (e), groundwater salinity (f).**

The proposed approach will use updated data sources and collect data and develop methods to assess MAR potential in confined sections of the main alluvial aquifer systems.

Gonzalez et al. (2020) identified potentially viable areas for MAR and considered proximity to a recharge water source (major river), and demand (irrigated agriculture) (Figure 22). Order of magnitude level estimates of potential aquifer storage volumes were made based on a broad assumption of unconsolidated aquifer storativity, and a minimal unsaturated zone thickness. The main advancement of the proposed methodology compared to the 2020 study, is transitioning from deterministic estimates based on uniform assumptions, to stochastic estimations of storage areas and potential volumes. This would enable answering questions such as:

- *What is the probability that MAR is feasible in an area?*
- *Where is MAR most likely to be feasible?*
- *What areas are feasible for MAR at a given confidence level?*
- *What is the expected range of available aquifer storage volumes in an area?*
- *What is the likely storage volume in an area at a given confidence level?*

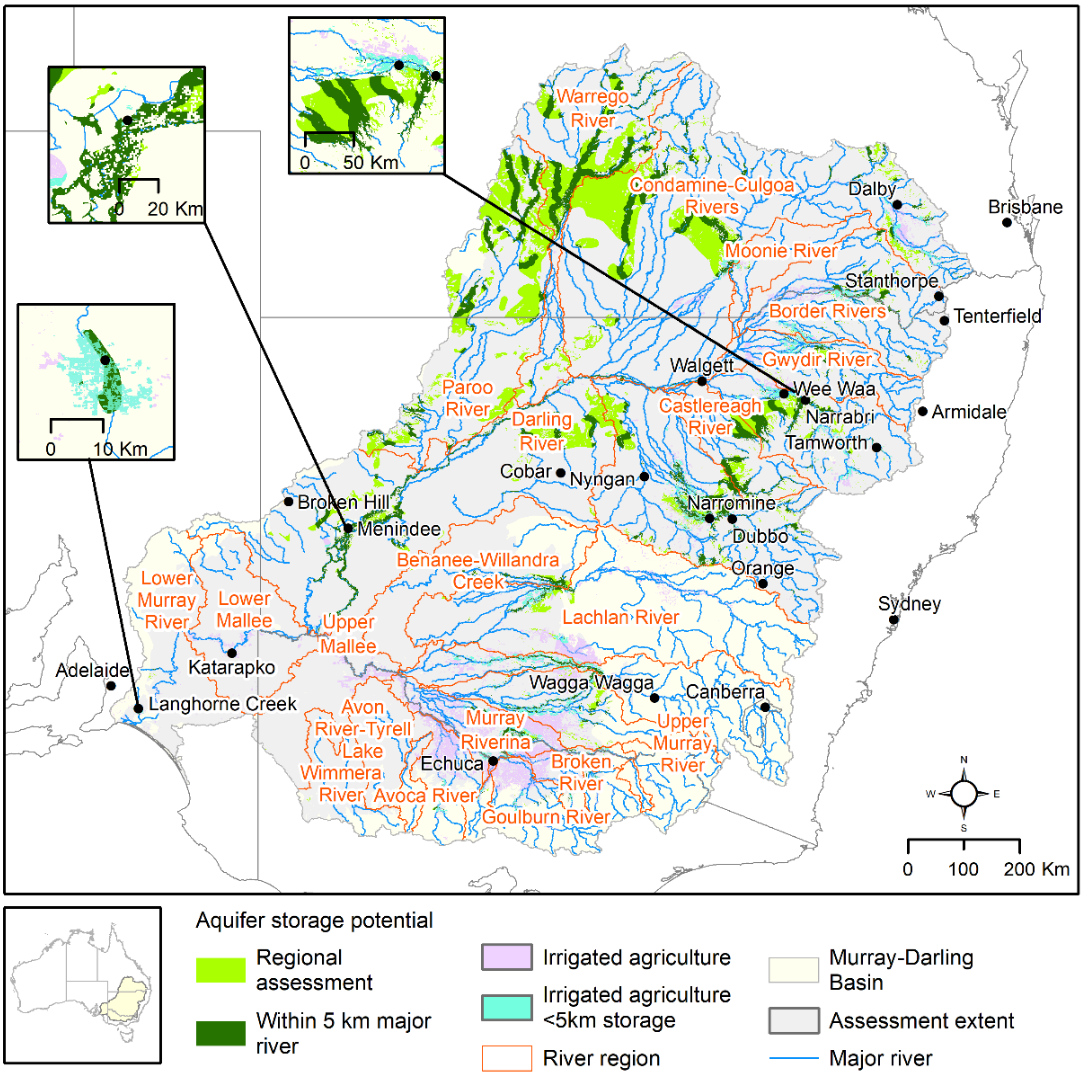

Figure 22 Murray–Darling Basin (MDB) regional aquifer storage potential in alluvium, colluvium, and sand plain aquifers where clay content < 40%, slope < 10%, regolith thickness > 10 m, water table depth > 5 m, and groundwater < 3000 mg/L, and within 5 km of major watercourses and irrigated agriculture (Gonzalez et al., 2020).

4.2 Framework proposed

Uncertainty in estimated MAR potential will be captured by using Monte Carlo thresholds for spatial criteria to map constraints (Figure 23). The assessment will use a gridded, spatial screening approach and focus on several key criteria that determine MAR potential for each grid cell across main alluvial SDL resource units (Figure 1). For unconfined aquifers sections of these systems criteria include:

1. Topographic slope
2. Soil clay content and as indicator of permeability
3. Aquifer presence and lateral extent (SDL resource areas)
4. Aquifer vertical thickness (model data or regolith thickness product)
5. Water table height (e.g., interpolated from groundwater level trend analysis data)
6. Groundwater salinity (e.g., interpolated from bore observations, Figure 3)
7. Some measure of groundwater productivity e.g. to represent potential bore yields

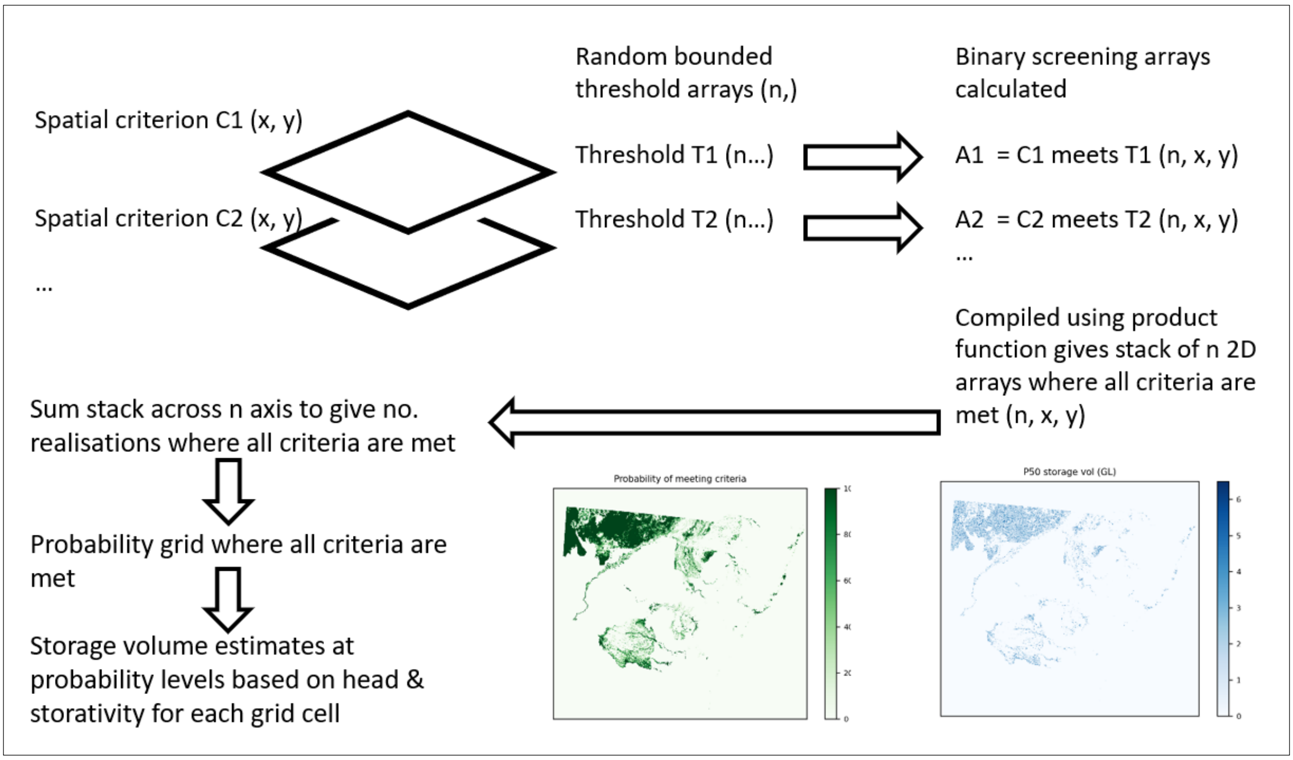

Figure 23 Stochastic mapping process for assessing MAR potential (map panels use synthetic data for illustrative purposes)

For confined aquifers, criteria related to infiltration potential are irrelevant and the assessment focusses on:

1. Aquifer presence and lateral extent (SDL resource areas)
2. Aquifer vertical thickness (model data or regolith thickness product
3. Piezometric head (interpolated from groundwater level trend analysis data)

4. Groundwater salinity (e.g., interpolated from bore observations, Figure 3)
5. Some measure of groundwater productivity to represent potential bore yields

The methodology requires input data represented on a uniform assessment grid, i.e., matched extent and resolution. A spatial resolution equivalent to 9 arc seconds (~250 m) is considered appropriate for this level of analysis and expected spatial precision and accuracy of input data. Criteria are passed through a bounded array of thresholds to generate stacks of Boolean arrays that are combined through a product function resulting in multiple grid realisations representing areas where all criteria are met (Figure 18). Derivative grids are calculated from probability of meeting criteria, e.g., storage volume estimates at given probability levels based on unsaturated zone thickness (unconfined aquifers), piezometric head (confined aquifers), and storativity (effective porosity in unconfined aquifers, specific storage in confined aquifers).

4.3 Preliminary results

The assessment coding framework is complete however synthetic data are being used as placeholders to test the analysis and draft figures and summary results. The first output is a grid showing the proportion of realisations where all criteria are met. Preliminary results are shown in Figure 24 for unconfined aquifers. This map highlights the areas where infiltration-based MAR is most likely to be feasible according to the criteria and threshold ranges used (noting these results contain synthetic data for illustration).

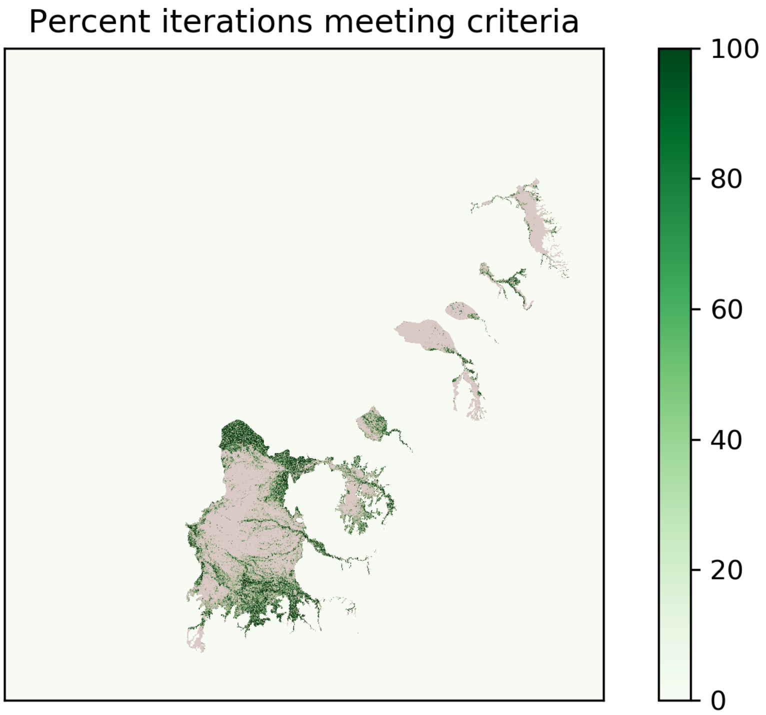

Figure 24 Probability of meeting all criteria for infiltration-based MAR potential in unconfined areas across the main alluvial SDL resource units in the MDB. Results are preliminary and contain synthetic data for illustration

Results can also be summarised by total area meeting all criteria at different ‘confidence’ levels, e.g., 65,000 km^2, 32,000 km^2 and 13,000 km^2 where criteria are met 10%, 50% and 90 % of the time respectively. These totals can also be disaggregated to summarise results at SDL resource unit level and be screened to consider proximity to water courses or irrigated areas (areas of potential sources for recharge and demand for water).

The second set of outputs are grids showing potential storage volumes at different confidence levels across the study area. An example using synthetic data is shown in Figure 25 for storage volumes in unconfined aquifers at the 50% confidence level (where 50% of realisations meet all criteria). Results are expressed in GL per grid cell (resolution of ~255 m) and are a product of the grid cell area meeting criteria, the height of the available unsaturated zone (or storage space), and effective porosity estimates.

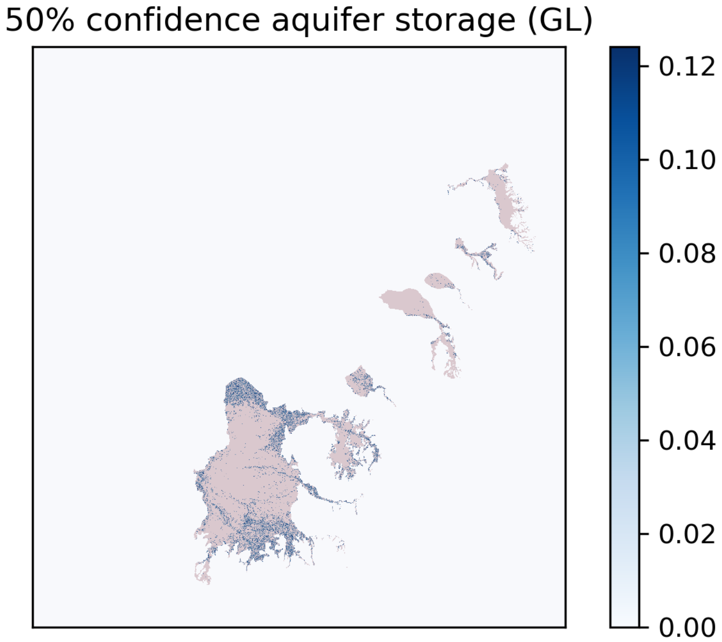

Figure 25 Estimated storage volume (GL) per grid cell at 50% confidence level for unconfined aquifers in the main alluvial SDL resource units in the MDB. Results are preliminary and contain synthetic data for illustration

Total volume estimates at different 'confidence' levels can be made and aggregated to summarise results at SDL resource unit level. Results can also be screened to consider proximity to water courses or irrigated areas (potential recharge water sources and demands for stored water).

5 Evaporation savings by implementing MAR

5.1 Scope

The objective of this section is to provide quantitative insights regarding the degree to which aquifer storage accessed through infiltration basins offers evaporative savings compared to equivalent surface storage. In this section we explore how evaporative losses through aquifer and surface storage change according to location, climate, and scheme scales and conditions.

Cumulative evaporative losses as a proportion of cumulative diverted volumes from a given water source (e.g., river) through infiltration basins and aquifer storage and dam storage will be compared. Outcomes of the study can inform where MAR can offer most potential savings and under which scales and conditions. This analysis contributes to the foundational analysis of MAR assessment and feasibility, for a posterior fully-fledged assessment of economic benefits of costs of implementing MAR.

5.2 Methodology and assumptions

The proposed approach involves water balance simulations using hydrological time series to trigger water diversion to aquifer and dam storage. Evaporation time series, matched to the corresponding discharge time series are used to calculate losses during infiltration or surface storage. A range of infiltration basin and dam configurations are simulated based on conditions in different climate zones across the main alluvial aquifers of the MDB.

The approach makes several general assumptions:

1. A monthly time step where river diversion, aquifer recharge and any losses are calculated for each month
2. Annual scheme capacity (target recharge or diversion volume) is determined assuming the target volume is achieved during 6 out of 12 months each year
3. Infiltration recharge rate (m/month) is based on daily rate (m/day) and assumed to occur over 15 days in the month when triggered
4. Target volume is diverted when river discharge exceeds set quantile value (trigger)
5. Infiltration basin area is a function of target volume, infiltration rate and a factor of 0.4 to approximate a 3:1 basin side batter slope
6. Basin evaporation losses occur during infiltration over 15 d/month when triggered, monthly evaporation based on time series calculated across the basin area
7. Same target volume is diverted to dam and evaporation loss occurs whenever there is positive water balance in dam based on the surface area to volume relationship for the given dam configuration
8. Simulations assume no rainfall inflow, and no other outflows, e.g., water use, aquifer losses or dam seepage loss

Data sources include:

- Long term river discharge time series from hydrological reference stations.
- Patch point Morton's Lake evaporation data for open water evaporation from the SILO database for the nearest available station.
- Dam surface area (SA) to volume (V) relationships for corresponding storages based on modelled and observed data.

It is proposed to replicate the analysis for multiple locations in the MDB targeting the main alluvial aquifer systems that represent different climate and hydrological conditions and corresponding dam configurations. Each location will simulate a range of infiltration basin capacities and infiltration rates.

5.3 Preliminary results

The calculations rely on surface area to volume (SA:V) relationships for the estimation of potential evaporation. For infiltration basins this is simply a function of the target capacity and infiltration rate, and a generic basin design that assumes 3:1 batter slope approximated using a factor of 0.4. For surface storage dams, the SA:V is derived using curves fitted to modelled area and volumes for Australian dam used in the AWRA-R v5.0 model (Dutta et al., 2015). In the case of Lake Keepit, a power function produces a fit with an R^2> 0.99 (Figure 26). This equation is used in the evaporation calculations to determine the area of the dam at any given volume.

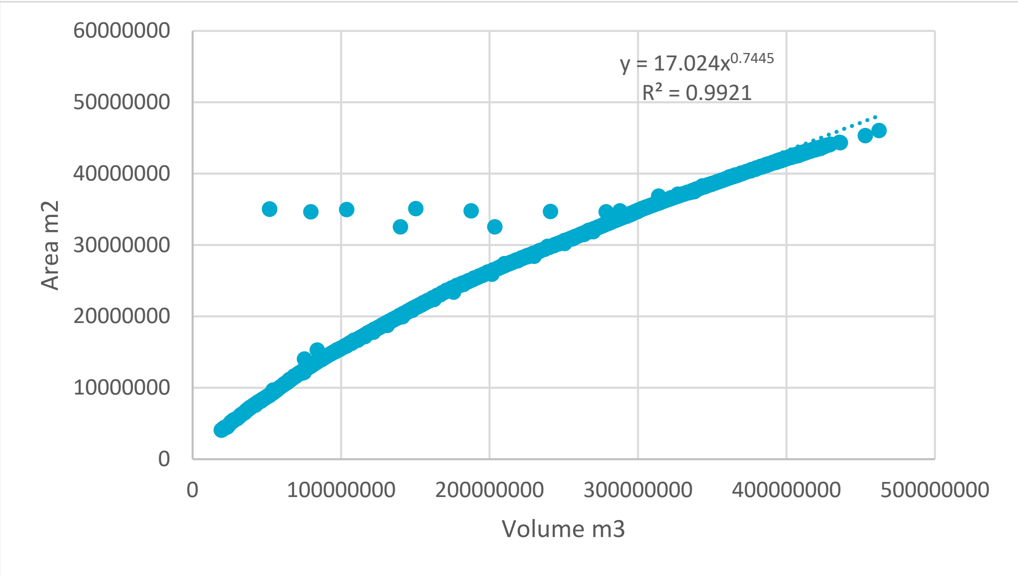

Figure 26 Surface area to volume (SA:V) relationship for Lake Keepit derived from the AWRA-R v5 model

A reference case using a typical farm dam configuration is used to compare modelled dam SA:V and associated evaporation. This is based on a review of farm dam volumes and surface areas in Australia (Lowe et al., 2005) where an equation to derived area from volume could be obtained as shown in Figure 27.

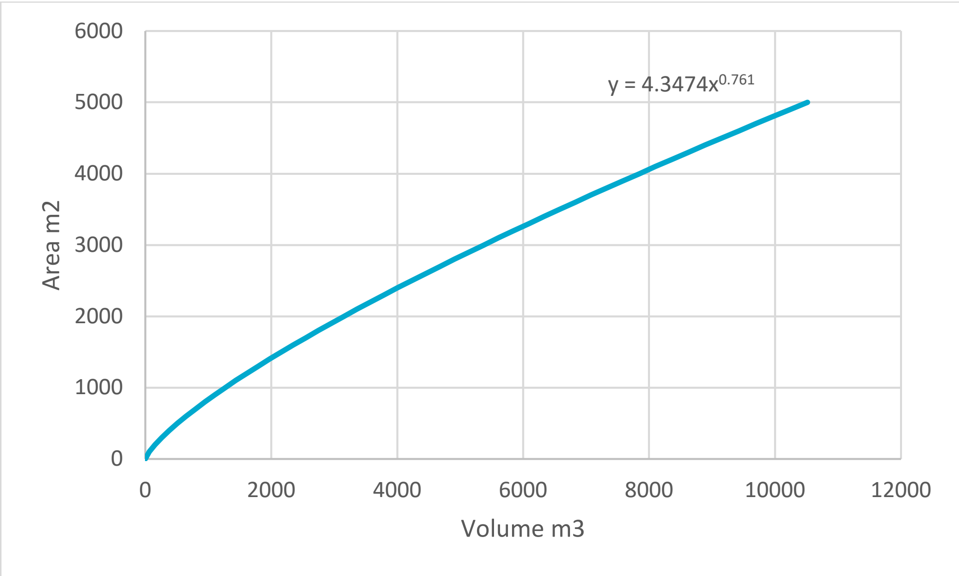

Figure 27 Volumes and surface areas of farm dams in Australia (equation derived from Lowe et al. 2005).

Comparing the slopes and equations above it is notable that the farm dam slope is slightly steeper than that of Lake Keepit. Lake Keepit will therefore have higher average SA:V and more evaporation loss for the same volume held compared to farm dam storage in evaporation calculations.

Preliminary evaporation results are given in Figure 28 for an example comparing an infiltration basin with a target capacity of 1 GL/y and infiltration rate of 0.5 m/d with equivalent storage in Lake Keepit and a typical farm dam. Of the 72.2 GL diverted over the time series, 71.7 GL was recharged with a total loss to evaporation during recharge of 500 ML, less than 1% of the volume diverted. In contrast, storing the same diverted volumes in surface storages with the SA:V characteristics of either Lake Keepit or a typical farm dam results in significant evaporation losses. Of the same total volume diverted, around 2 GL and 4 GL is held in storage at the end of the time series in the Lake Keepit and farm dam storages respectively. Evaporative losses total 70 GL and 68 GL or 98% and 94% of the volumes diverted respectively.

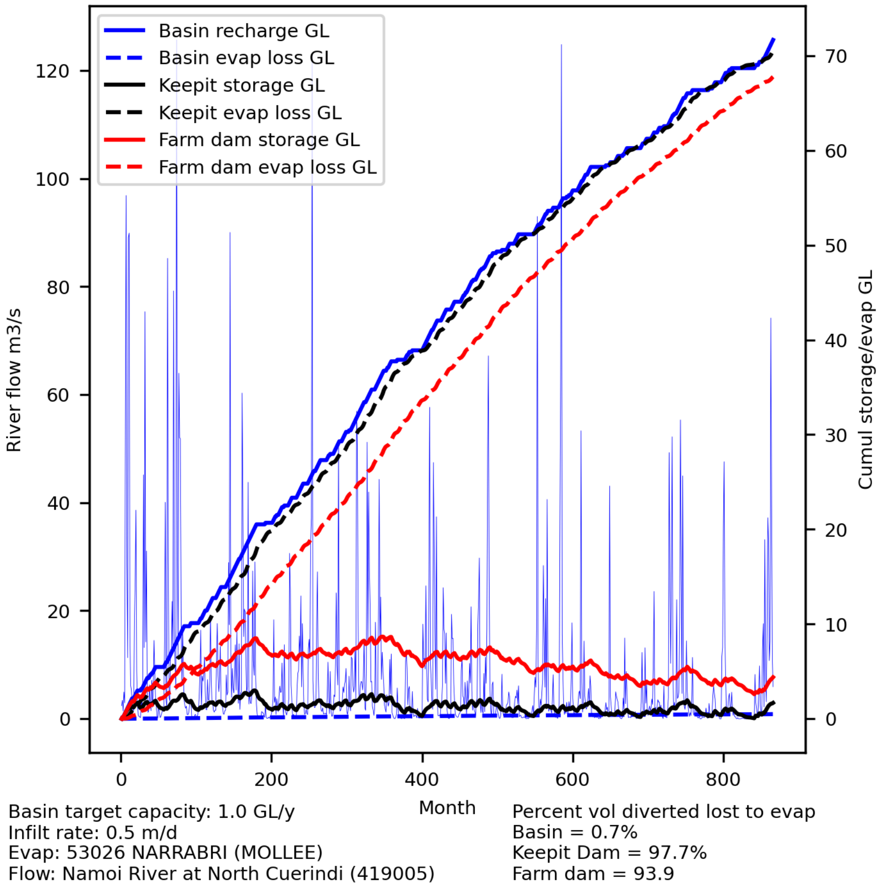

Figure 28 Evaporation losses comparing an infiltration basin with a target capacity of 1 GL/y and infiltration rate of 0.5 m/d with equivalent storage in Lake Keepit and a typical farm dam design. Diversion triggered at 50% flow exceedance on the Namoi River (419005) and Morton Lake evaporation data from Narrabri (53026)

If the same scenario is run assuming a basin infiltration rate of 0.1 m/d (instead of 0.5 m/d), greater evaporation losses are experienced during recharge, however, these remain an order of magnitude lower than Lake Keepit and farm dam losses (Figure 29). Basin losses total 2.5 GL or 3.4% of the diverted volume.

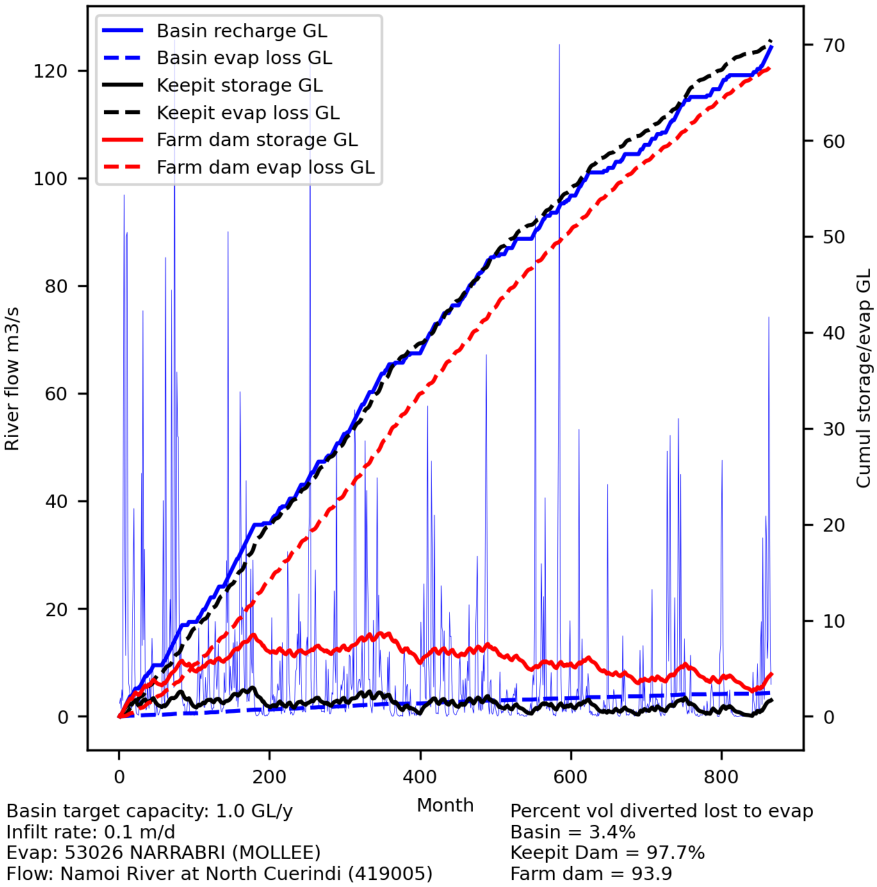

Figure 29 Evaporation losses comparing an infiltration basin with a target capacity of 1 GL/y and infiltration rate of 0.1 m/d with equivalent storage in Lake Keepit and a typical farm dam design. Diversion triggered at 50% flow exceedance on the Namoi River (419005) and Morton Lake evaporation data from Narrabri (53026)

6 Concluding remarks and next steps

Integrated assessment in the main alluvial aquifers of the MDB shows that eleven groundwater resource units used to manage these aquifer systems face aquifer resilience, stress and sustainability issues. The severity of these issues depends on local conditions and thus the assessment provides valuable insights on where to potentially concentrate efforts to improve groundwater management in the MDB to target specific issues such as declining groundwater levels, groundwater salinity or GDEs consideration.

The clustering analysis determined six dominant clusters explaining the main trends in historical (1971-2021) groundwater levels. Interpretation of each of these patterns indicates how the groundwater time series in each cluster behaved before, during and after the Millennium Drought. The two clustering methods, hierarchical clustering analysis (HCA) and the self-organising map (SOM) produced similar patterns with comparable numerical performance (MSE), indicating these six dominant patterns have been properly identified from the data set (910 observations bores). A difference arose in the number of time series which were allocated to each cluster, however a geographical analysis indicated that this was the result of time series within specific areas being attributed to closely-related patterns. The cluster-based geographic analysis also showed the Namoi and Gwydir region to have groundwater levels generally declining pre- and during the Millennium Drought with an evening-out afterwards, and bores in the Lachlan, Murrumbidgee, Murray and Goulburn region generally showed stable or increasing groundwater levels pre-drought, followed by a decline and a partial post-drought recovery.

A causal attribution framework is being developed to determine the main contributors to groundwater level changes in each region. This involves representing each region with a neural network model that can simulate changes in groundwater levels given certain climate and anthropogenic conditions. Once these models are developed, they can be probed to determine which driving factors are impacting the groundwater levels the most, using a mixture of visual and computational methods. It is possible to investigate these attributions temporally as well as spatially (including vertically), to determine if the main factors contributing to altered groundwater levels have transformed over the period of study. Accessing spatially and temporarily comprehensive data on groundwater use will largely determine the quality of the causal inference under anthropogenic conditions.

The preliminary results of the MAR potential mapping assessment illustrated the types of outputs generated with the assessment methodology for unconfined aquifer conditions. A modification of this methodology will be developed for confined aquifer conditions as described in 4.2. This will exclude criteria associated with infiltration potential and focus on aquifer properties. Storage assessments will be based on assuming additional storage would not result in creating artesian conditions. One of the key input data to both confined and unconfined assessment is the available height for recharge and storage. Previously this was done through basic interpolation of groundwater level data, e.g., median levels in bores since year 2000, and assumptions that recharge should not induce a water table rise beyond a certain level to avoid issues at the surface (Gonzalez et al., 2020). The current study will test the feasibility of using groundwater level trend magnitudes (e.g. described in Section 3) as a basis for spatial interpolation. This will capture temporal dynamics in groundwater levels and avoid assumptions of maximum allowable water level rise. In areas where groundwater has been in long-term decline, it can instead be assumed that the upper limit for MAR would be the historical level prior to intensive extraction.

Results of the evaporation calculations indicated the potential savings that could be realised by using sub-surface storage (infiltration basins) in locations where there is a suitable aquifer and where surface storage configurations, either existing or proposed, have limited efficiency due to high SA:V relationships and high evaporation potential. Replication of these calculations in different areas with a range of conditions and configurations will yield more insights into where MAR can offer potential benefits. It should be noted however, that the results presented here overestimate actual evaporative losses from surface storage as usage is not factored. If water was stored in a dam for a period and then used, the used volume would not be subject to evaporation loss and the proportion of total diverted water lost would be reduced. Evaporation losses reported here should not therefore be interpreted as potential losses from reservoirs or farm dams under normal operation. Water stored in aquifers may also be subject to reduction through hydraulic loss or water quality limitations not considered here. Similarly, extraction of stored water could reduce actual losses over time and to account for this demand should be considered.

In the third year, RQ8b research will focus on consolidating our understanding of MAR as an operational adaptation option to water management in the MDB. Planned activities include proposing and exploring a framework for economic assessment to reduce uncertainty around the costs of MAR at different scales and operating conditions. The results of the resilience, stress and sustainability assessment, in combination with mapping of MAR potential will be used to develop one or more conceptual MAR site configurations for estimating the costs of implementing a MAR scheme in a proposed location. To contextualise the assessment, the policy and regulatory principles and framework needed to enable the implementation of MAR will be explored. This will depend on the scale and objective of the conceptualised scheme, and potential ownership and governance arrangements.

References

Akbar, H., Nilsalab, P., Silalertruksa, T., & Gheewala, S. H. (2022). Comprehensive review of groundwater scarcity, stress and sustainability index-based assessment. *Groundwater for Sustainable Development*, *18*(December 2021), 100782. https://doi.org/10.1016/j.gsd.2022.100782

Barron, O., Crosbie, R., Charles, S., Dawes, W., Ali, R., Evans, W., Cresswell, R., Pollock, D., Hodgson, G., Currie, D., Mpelasoka, F., Pickett, T., Aryal, S., Donn, M., & Wurcker, B. (2011). Climate change impact on groundwater resources in Australia. In *Waterlines Report* (Vol. 2011). http://archive.nwc.gov.au/library/waterlines/67

Breiman, Leo. "Random forests." *Machine learning* 45 (2001): 5-32.

Butler, A. P. (2010). Groundwater vulnerability and protection. In H. Wheater, S. Mathias, & X. Li (Eds.), *Groundwater Modelling in Arid and Semi-Arid Areas* (pp. 75–86). Cambridge University Press. https://doi.org/10.1017/CBO9780511760280.007

Clark, S. R. (2022). Unravelling groundwater time series patterns: Visual analytics-aided deep learning in the Namoi region of Australia. *Environmental Modelling and Software*, *149*(September 2021), 105295. https://doi.org/10.1016/j.envsoft.2022.105295

Currie, D., Wiltshire, E., Irvine, E., Evans, W. R., Barron, O., & Cresswell, R. (2010). *Investigating the Impact of Climate Change on Groundwater* (Issue November). papers2://publication/uuid/312D6CB7-C0F1-4B3D-BEFE-134AF0937B8A

de la Hera-Portillo, Á., López-Gutiérrez, J., Mayo, B., López-Gunn, E., Henriksen, H. J., Gejl, R. N., Zorrilla-Miras, P., & Martínez-Santos, P. (2021). An initial framework for understanding the resilience of aquifers to groundwater pumping. *Water (Switzerland)*, *13*(4), 1–15. https://doi.org/10.3390/w13040519

DNRME. (2018). *Upper Condamine Alluvium Central Condamine Alluvium Groundwater Background Paper*. https://www.mdba.gov.au/sites/default/files/pubs/qld-central-condamine-alluvium-%28GS64a%29-groundwater-background-paper-2018_1.pdf

Dong, Z., Jia, W., Sarukkalige, R., Fu, G., Meng, Q., & Wang, Q. (2020). Innovative trend analysis of air temperature and precipitation in the jinsha river basin, china. *Water (Switzerland)*, *12*(11). https://doi.org/10.3390/w12113293

Dutta, D., Kim, S., Hughes, J., Vaze, J., & Yang, A. (2015). *AWRA-R v5.0*. https://publications.csiro.au/rpr/download?pid=csiro:EP154523&dsid=DS2

Elshall, A. S., Arik, A. D., El-Kadi, A. I., Pierce, S., Ye, M., Burnett, K. M., Wada, C. A., Bremer, L. L., & Chun, G. (2020). Groundwater sustainability: A review of the interactions between science and policy. *Environmental Research Letters*, *15*(093004). https://doi.org/10.1088/1748-9326/ab8e8c

Fu, G., Chiew, F. H. S., & Post, D. A. (2023). Trends and variability of rainfall characteristics influencing annual streamflow: A case study of southeast Australia. *International Journal of Climatology*, *43*(3), 1407–1430. https://doi.org/10.1002/joc.7923

Fu, G., Rojas, R., & Gonzalez, D. (2022). Trends in Groundwater Levels in Alluvial Aquifers of the Murray–Darling Basin and Their Attributions. *Water*, *14*(11), 1808. https://doi.org/10.3390/w14111808

Gleeson, T., Cuthbert, M., Ferguson, G., & Perrone, D. (2020). Global Groundwater Sustainability, Resources, and Systems in the Anthropocene. *Annual Review of Earth and Planetary Sciences*, *48*, 431–463. https://doi.org/10.1146/annurev-earth-071719-055251

Gleeson, T., Wada, Y., Bierkens, M. F. P., & van Beek, L. P. H. (2012). Water balance of global aquifers revealed by groundwater footprint. *Nature*, *488*(7410), 197–200. https://doi.org/10.1038/nature11295

Gonzalez, D., Dillon, P., Page, D., & Vanderzalm, J. (2020). The Potential for Water Banking in Australia's Murray–Darling Basin to Increase Drought Resilience. *Water*, *12*(10), 2936. https://doi.org/10.3390/w12102936

Gorelick, R. (2006). Combining richness and abundance into a single diversity index using matrix analogues of Shannon's and Simpson's indices. *Ecography*, *29*, 525–530.

Hart, B. T., Bond, N. R., Byron, N., Pollino, C. A., & Stewardson, M. J. (2020). Introduction to the Murray–Darling Basin system, Australia. In B. T. Hart, N. R. Bond, N. Byron, C. A. Pollino, & M. J. Stewardson (Eds.), *Murray-Darling Basin, Australia: Its Future Management* (1st ed., Vol. 1, pp. 1–17). Elsevier Inc. https://doi.org/10.1016/b978-0-12-818152-2.00001-2

Hirsch, R. M., Slack, J. R., & Smith, R. A. (1982). Techniques of trend analysis for monthly water quality data. *Water Resources Research*, *18*(1), 107–121. https://doi.org/10.1029/WR018i001p00107

Kendall, M. G. (1975). *Rank Correlation Methods* (4th ed.). Charles Griffin.

Kohonen, T. (1990). The self-organizing map. *Proceedings of the IEEE*, *78*(9), 1464–1480. https://doi.org/10.1109/5.58325

Kourgialas, N. N., Karatzas, G. P., Dokou, Z., & Kokorogiannis, A. (2018). Groundwater footprint methodology as policy tool for balancing water needs (agriculture & tourism) in water scarce islands - The case of Crete, Greece. *Science of The Total Environment*, *615*, 381–389. https://doi.org/10.1016/j.scitotenv.2017.09.308

Leblanc, M., Tweed, S., van Dijk, A., & Timbal, B. (2012). A review of historic and future hydrological changes in the Murray-Darling Basin. *Global and Planetary Change*, *80–81*, 226–246. https://doi.org/10.1016/j.gloplacha.2011.10.012

Lowe, L., Nathan, R., & Morden, R. (2005). Assessing the impact of farm dams on streamflows, Part II: Regional characterisation. *Australasian Journal of Water Resources*, *9*(1), 13–26. https://doi.org/10.1080/13241583.2005.11465260

Mahdavi, T. (2021). Evaluation of quantitative and qualitative sustainability of aquifers by groundwater footprint methodology: case study: West Azerbaijan Province, Iran. *Environmental Monitoring and Assessment*, *193*(368), 1–18. https://doi.org/10.1007/s10661-021-09142-7

Majidipour, F., Najafi, S. M. B., Taheri, K., Fathollahi, J., & Missimer, T. M. (2021). Index-based Groundwater Sustainability Assessment in the Socio-Economic Context: a Case Study in the Western Iran. *Environmental Management*, *67*(4), 648–666. https://doi.org/10.1007/s00267-021-01424-7

McNeil, V. H., Raymond, M. A. A., Bennett, L., McGregor, G. B., & Southwell, B. (2018). *Regional groundwater chemistry zones: Queensland Murray-Darling Basin*. https://environment.des.qld.gov.au/__data/assets/pdf_file/0024/90771/regional-groundwater-chemistry-zones-qld-murray-darling-basin.pdf

MDBA. (2020a). *Groundwater report cards For Sustainable Diversion Limit Resource Units under the* (Issue November). Murray-Darling Basin Authority.

MDBA. (2020b). *Transition Period Water Take Report 2018/19*.

Mukherjee, P., Singh, C. K., & Mukherjee, S. (2012). Delineation of Groundwater Potential Zones in Arid Region of India-A Remote Sensing and GIS Approach. *Water Resources Management*, *26*(9), 2643–2672. https://doi.org/10.1007/S11269-012-0038-9

Nielsen, F. (2016). Hierarchical Clustering. In *Introduction to HPC with MPI for Data Science* (pp. 195–211). Springer Cham. https://doi.org/10.1007/978-3-319-21903-5_8

NSW DPI. (2018a). *Gwydir Alluvium Water Resource Plan – Groundwater Resource Description.*

NSW DPI. (2018b). *Lachlan Alluvium Water Resource Plan - Groundwater Resource Description*. https://www.industry.nsw.gov.au/__data/assets/pdf_file/0010/175969/Lachlan-alluvium-appendice-a-water-resource-description.pdf

NSW DPI. (2018c). *Macquarie-Castlereagh Alluvium Water Resource Plan - Groundwater Resource Description*. https://www.industry.nsw.gov.au/__data/assets/pdf_file/0017/192221/macquarie-castlereagh-alluvium-appendix-a-water-resource-description.pdf

NSW DPI. (2019a). *Murray Alluvium Water Resource Plan - Groundwater Resource Description*. https://www.industry.nsw.gov.au/__data/assets/pdf_file/0004/230674/appendix-a-murray-alluvium-wrp-groundwater-resource-description.pdf

NSW DPI. (2019b). *Namoi Alluvium Water Resource Plan - Groundwater Resource Description*. https://www.industry.nsw.gov.au/__data/assets/pdf_file/0017/230804/Namoi-Alluvium-WRP-resource-description.pdf

NSW-DPIE. (2019a). *NSW Border Rivers Alluvium Water Resource Plan - Groundwater Resource Description*. https://www.industry.nsw.gov.au/__data/assets/pdf_file/0020/236072/appendix-a-nsw-border-rivers-alluvium-gw-resource-description.pdf

NSW-DPIE. (2019b). *The Basin Plan implementation - Murrumbidgee Alluvium Water Resource Plan Resource Description*. https://www.industry.nsw.gov.au/__data/assets/pdf_file/0017/313127/appendix-a-murrumbidgee-alluvium-wrp-groundwater-resource-description.pdf

OGIA. (2016). *Groundwater connectivity between the Condamine Alluvium and the Walloon Coal Measures A hydrogeological investigation report*. https://www.resources.qld.gov.au/__data/assets/pdf_file/0019/403282/condamine-report-hydrogeological-investigation.pdf

Page, D., Vanderzalm, J., Gonzalez, D., Castellazzi, P., Bennet, J., Barron, O., & Peake, A. (2021). *Rapid appraisal of Managed Aquifer Recharge (MAR) opportunities for agriculture*. https://doi.org/10.25919/bbzw-qw50

Richey, A., Thomas, B. F., Lo, M.-H., Famiglietti, J. S., Swenson, S., & Rodell, M. (2015). Uncertainty in global groundwater storage estimates in a Total Groundwater Stress framework. *Water Resources Research*, *51*, 5198–5216. https://doi.org/10.1111/j.1752-1688.1969.tb04897.x

Richey, A., Thomas, B. F., Lo, M.-H., Reager, J. T., Famiglietti, J. S., Voss, K., Swenson, S., & Rodell, M. (2015). Quantifying renewable groundwater stress with GRACE. *Water Resources Research*, *51*, 5217–5238. https://doi.org/10.1002/2015WR017349

Rine, J. M., Shafer, J. M., Covington, E., Berg, R. C., Rine, J. M., Shafer, J. M., Covington, E., & Berg, R. C. (2006). Testing of stack-unit/aquifer sensitivity analysis using contaminant plume distribution in the subsurface of Savannah River Site, South Carolina, USA. *Hydrogeology Journal*, *14*, 1620–1634. https://doi.org/10.1007/s10040-006-0083-7

Rojas, R., Gonzalez, D., & Fu, G. (2023). Resilience, stress and sustainability of alluvial aquifers in the Murray-Darling Basin, Australia: Opportunities for groundwater management. *Journal of Hydrology: Regional Studies*, 47 (2023) 101419.

Ross, A. (2012). Easy to say, hard to do: Integrated surface water and groundwater management in the Murray-Darling Basin. *Water Policy*, *14*(4), 709–724. https://doi.org/10.2166/wp.2012.129

Şen, Z. (2012). Innovative Trend Analysis Methodology. *Journal of Hydrologic Engineering*, *17*(9), 1042–1046. https://doi.org/10.1061/(asce)he.1943-5584.0000556

Smakhtin, V., Revenga, C., & Döll, P. (2004). A Pilot Global Assessment of Environmental Water Requirements and Scarcity. *Water International*, *29*(3), 307–317. https://doi.org/10.1080/02508060408691785

Spellerberg, I. F., & Fedor, P. J. (2003). A tribute to Claude Shannon (1916-2001) and a plea for more rigorous use of species richness, species diversity and the "Shannon-Wiener" Index. *Global Ecology & Biogeography*, *12*, 177–179. http://www.blackwellpublishing.com/journals/geb

Stewardson, M. J., Walker, G., & Coleman, M. (2021). Hydrology of the Murray–Darling Basin. In B. T. Hart, N. Byron, M. J. Stewardson, N. R. Bond, & C. A. Pollino (Eds.), *Murray-Darling Basin, Australia* (1st ed., Vol. 1, pp. 47–73). Elsevier Inc. https://doi.org/10.1016/b978-0-12-818152-2.00003-6

VIC-DELWP. (2020). *Groundwater-Surface Water Interaction (Lines)*. Spatial Dataset. https://data.aurin.org.au/dataset/vic-govt-delwp-datavic-water-gw-sw-interaction-na

Walker, G., Barnett, S., & Richardson, S. (2020). Developing a Coordinated Groundwater Management Plan for the Interstate Murray-Darling Basin. In J. M. Rinaudo, C. Holley, S. Barnett, & M. Montginoul (Eds.), *Sustainable Groundwater Management: A Comparative Analysis of French and Australian Policies and Implications to Other Countries* (Vol. 24, pp. 143–161). Springer. https://doi.org/10.1007/978-3-030-32766-8_8

Water, G.-M. (2015). *Shepparton Irrigation Region Groundwater Management Area - Local Management Plan*. https://www.g-mwater.com.au/downloads/gmw/Groundwater/Shepparton_Irrigation_Region_WSPA/29022016_-_3786511-v25-SHEPPARTON_IRRIGATION_REGION_GROUNDWATER_LOCAL_MANAGEMENT_PLAN.pdf

Watson, A., Peterson, E. W., Malone, D., & Tranel, L. (2020). Geology and Aquifer Sensitivity of Quaternary Glacial Deposits Overlying a Portion of the Mahomet Buried Bedrock Valley Aquifer System. *Hydrology*, *7*(69), 1–18. https://doi.org/10.3390/hydrology7040069

Welsh, W., Herron, N., Rohead-O'Brien, H., Cook, S., Aryal, S., Mitchell, P., Ransley, T., & Cassel, R. (2014). *Context statement for the Namoi subregion. Product 1.1 for the Northern Inland Catchments Bioregional Assessment* (Issue June).

Welsh, W., Herron, N., Rohead-O'Brien, H., Ransley, T., Aryal, S., Mitchell, P., Buckerfield, S., & Marshall, S. (2014). *Context statement for the Maranoa-Balonne-Condamine subregion. Product 1.1 for the Maranoa-Balonne-Condamine from the Northern Inland Catchments Bioregional Assessment*. file:///C:/Users/roj008/AppData/Local/Temp/1.1 Context statement for the Maranoa-Balonne-Condamine subregion-3.pdf

Wilford, J., Ross, S., Thomas, M., & Grundy, M. (2018). *Soil and Landscape Grid National Soil Attribute Maps - Depth of Regolith (3" resolution) - Release 2*. V6. CSIRO. Data Collection. https://doi.org/10.4225/08/55C9472F05295

Williams, J. (2011). Understanding the Basin and its Dynamics. In D. Connell & Q. Grafton (Eds.), *Basin Futures: Water reform in the Murray-Darling Basin* (First, pp. 1–37). ANU Press. https://doi.org/10.22459/BF.05.2011

Appendices

Table A.1 Metered groundwater annual actual take reported in (MDBA, 2020b)**. BDL: Baseline Diversion Limit and SDL: Sustainable Diversion Limit as defined in Schedule 4 of the Basin Plan**

SDL code	SDL name			Annual actual take (GL/y)							Annual actual take GL/y 2012-2019		
		BDL (GL/y)	SDL (GL/y)	2012-13	2013-14	2014-15	2015-16	2016-17	2017-18	2018-19	Max	Min	Average
GS64a	Upper Condamine Alluvium (Central Condamine Alluvium)	81.4	46.0	32.3	55.1	41.1	42.0	48.0	50.5	57.7	57.7	32.3	46.7
GS64b	Upper Condamine Alluvium (Tributaries)	45.5	40.5	33.9	32.9	30.6	32.6	32.8	33.7	35.6	35.6	30.6	33.2
GS54	Queensland Border Rivers Alluvium	14.0	14.0	8.85	11.3	11.8	12.8	10.8	14.0	14.4	14.4	8.85	12.0
GS32	NSW Border Rivers Alluvium	8.40	8.40	2.84	5.59	5.41	3.98	3.38	6.37	8.98	8.98	2.84	5.22
GS33	NSW Border Rivers Tributary Alluvium	0.41	0.41	0.16	0.17	0.17	0.17	0.17	0.17	0.16	0.17	0.16	0.17
GS27a	Lower Murray Shallow Alluvium	81.9	81.9	2.26	4.10	5.90	5.40	5.97	8.39	11.9	11.9	2.26	6.27
GS27b	Lower Murray Deep Alluvium	88.9	88.9	56.2	45.2	67.5	85.5	36.7	78.9	110.7	110.7	36.7	68.7
GS46	Upper Murray Alluvium	14.1	14.1	12.3	10.7	9.87	11.2	8.66	14.0	17.8	17.8	8.66	12.1
GS28a	Lower Murrumbidgee Shallow Alluvium	26.9	26.9	5.25	6.47	7.15	6.21	6.47	8.17	8.32	8.32	5.25	6.86
GS28b	Lower Murrumbidgee Deep Alluvium	273.6	273.6	179.6	230.3	300.3	268.5	151.5	323.1	377.9	377.9	151.5	261.6
GS31	Mid-Murrumbidgee Alluvium	53.5	53.5	35.5	36.1	40.1	32.4	30.3	42.7	55.6	55.6	30.3	39.0
GS25	Lower Lachlan Alluvium	123.4	117.0	87.2	104.9	120.5	97.5	91.4	127.2	131.8	131.8	87.2	108.6
GS44	Upper Lachlan Alluvium	94.2	94.2	44.2	42.3	57.2	55.7	37.9	75.4	89.4	89.4	37.9	57.4
GS26	Lower Macquarie Alluvium	70.7	70.7	26.9	29.7	32.0	35.2	18.6	40.8	47.4	47.4	18.6	32.9
GS45	Upper Macquarie Alluvium	17.9	17.9	13.7	14.1	15.3	15.9	13.5	21.0	23.0	23.0	13.5	16.6
GS29	Lower Namoi Alluvium	88.3	88.3	61.1	104.3	105.1	93.0	51.2	95.3	116.2	116.2	51.2	89.5
GS47	Upper Namoi Alluvium	123.4	123.4	90.1	113.6	102.4	93.7	70.1	105.7	112.2	113.6	70.1	98.3
GS48	Upper Namoi Tributary Alluvium	1.77	1.77	0.55	0.38	0.21	0.23	0.18	0.28	0.19	0.55	0.18	0.29
GS24	Lower Gwydir Alluvium	33.0	33.0	29.3	46.4	43.3	35.5	23.8	35.5	37.5	46.4	23.8	35.9
GS43	Upper Gwydir Alluvium	0.72	0.72	0.07	0.07	0.07	0.07	0.12	0.07	0.07	0.12	0.07	0.08
GS8a	Goulburn-Murray: Shepparton Irrigation Region	244.1	244.1	41.3	35.5	43.7	79.5	54.2	43.4	96.3	96.3	35.5	56.3
GS8c	Goulburn-Murray: Sedimentary Plain	203.5	223.0	101.2	98.4	136.5	141.5	138.9	120.9	149.1	149.1	98.4	126.6

As Australia's national science agency and innovation catalyst, CSIRO is solving the greatest challenges through innovative science and technology.

CSIRO. Unlocking a better future for everyone.

Contact us

1300 363 400
+61 3 9545 2176
csiroenquiries@csiro.au
www.csiro.au

For further information

Land and Water
Dr Rodrigo Rojas
+61 **07 3833 5600**
Rodrigo.rojas@csiro.au
csiro.au/en/about/people/business-units/land-and-water